# Potassium-, Uranium- and Thorium-concentrations in bedrock

## A Study of the Sahlgrenska Anomaly and Änggårdsbergen, Gothenburg

**Frida Elf**
**Johanna Winberg**

**Degree of Bachelor of Science**
**with a major in Earth Sciences**
**15 hec**

**Department of Earth Sciences**
**University of Gothenburg**
**2019 B-1072**

Faculty of Science

UNIVERSITY OF GOTHENBURG

**UNIVERSITY OF GOTHENBURG**
**Department of Earth Sciences**
**Geovetarcentrum/Earth Science Centre**

# Potassium-, Uranium- and Thorium-concentrations in bedrock

## A Study of the Sahlgrenska Anomaly and Änggårdsbergen, Gothenburg

**Frida Elf**
**Johanna Winberg**

**ISSN 1400-3821**

**B1072**
**Bachelor of Science thesis**
**Göteborg 2019**

**Mailing address**
Geovetarcentrum
S 405 30 Göteborg

**Address**
Geovetarcentrum
Guldhedsgatan 5A

**Telephone**
031-786 19 56

Geovetarcentrum
Göteborg University
S-405 30 Göteborg
SWEDEN

**Acknowledgments**

This study would not have been possible without the valuable guidance from our precious source of knowledge, Professor Erik Sturkell. We have shared many funny moments these past two months, including rewarding discussions and laughter in front of youtube. We would like to give a huge thank you to Thomas Eliasson from SGU, who has provided us with essential information for field work and about the RA-granite. Thank you to our examiner Matthias Konrad-Schmolke for taking the time to read our study. Thank you, Mikael Tillberg for helping us out with microscopy and SEM, but also for showing us different angles on mineralogy for our study. Thank you Niclas Hultin who helped us not saw our fingers off when using the sawing laboratory at University of Gothenburg. We also want to thank our classmates Fredrik Andersson, Markus Settergren, Fanny Ekström and Tobias Möhl for constructive comments, these helped us a lot. At last, a gigantic thank you to all the curious nurses and doctors asking us questions when we were doing gamma spectrometry in the hospital area, the Swedish weather which actually gave us sun and the guy in the office next to Erik whose name we do not know but who were always ready with the key.

*"To beginnings… and endings, and the wisdom to know the difference."*

- *Twin Peaks*

## Abstract

This study investigates the RA-granite (also known as Kärra Granite), which form a north-south trending intrusive body traversing Gothenburg. The spatial distribution of the radioactive elements K, U and Th in RA-granite was measured in southern Gothenburg (Änggårdsbergen and Sahlgrenska University Hospital), Sweden. The 1311 Ma old intrusive RA-granite has high concentrations of U and Th. It is the dominating bedrock of Änggårdsbergen, Sahlgrenska University Hospital and parts of Medicinareberget. The area has been deformed during two major orogenies but the RA-granite has only been affected by the last orogeny, the Sweconorweigan orogeny. This study investigates concentrations in the areas mentioned above, with focus on Sahlgrenska University Hospital/Medicinareberget where an enrichment in Th and K has been found in previous studies, the so called Sahlgrenska anomaly. The aims of the report were to, via field studies, chemical and optical analysis, map the spatial distribution of K, U and Th – and to investigate in which minerals U and Th reside. The main focuses of the report were to discuss the possible extension of the Sahlgrenska anomaly, evidence of possible hydrothermal and tectonic events in this area. The spatial distribution of Th shows a local enrichment surrounding the Sahlgrenska anomaly and an increase of concentrations from east to west. Uranium has lower concentrations surrounding the anomaly. Potassium is enriched surrounding the Sahlgrenska anomaly but have normal granite values throughout the field area. The study has shown new normal values for the radioactive elements in RA-granite, 3.5-5 % K, 7-18 ppm U and 30-70 ppm Th. The U/Th ratios indicates a hydrothermal event both in parts of Änggårdsbergen but also surrounding the Sahlgrenska anomaly. The radioactive elements U and Th were found in accessory minerals zircon and titanite, both primary but also possibly secondary titanite. No biotite was found, but instead we found the typically hydrothermal mineral chlorite, so all biotite could have been chloritized. Allanite was found in previous studies but not in this study. The U/Th ratios indicates a hydrothermal event both in parts of Änggårdsbergen but also surrounding the Sahlgrenska anomaly. The conclusion of the report was that we now have normal values for the RA-granite, that hydrothermal events have taken place at the Sahlgrenska anomaly and tectonic implications were seen in the microscopy studies.

**Key words:** *RA-granite, uranium, potassium, thorium, hydrothermal alteration, Änggårdsbergen, Gothenburg, zircon*

## Sammanfattning

Denna rapport undersöker RA-graniten (även kallad Kärragranit), som formar en nord-sydligt liggande intrusion som korsar Göteborg. Den rumsliga fördelningen av de radioaktiva grundämnena K, U och Th i RA-graniten mättes i södra Göteborg (Änggårdsbergen och Sahlgrenska Universitetssjukhuset), Sverige. Den 1311 Ma år gamla RA-graniten innehåller höga halter av U och Th. RA-graniten är den dominerande bergarten i Änggårdsbergen, Sahlgrenska Universitetssjukhuset och delar av Medicinareberget. Området i sig har blivit deformerat under två orogeneser, men RA-graniten har endast påverkats av den senaste, den Svekonorvegiska orogenesen. Denna studie undersöker halterna i de tidigare nämnda områdena, med fokus på Sahlgrenska Universitetssjukhuset samt Medicinareberget där förhöjda halter av K och Th har hittats i tidigare studier, den så kallade Sahlgrenska-anomalin. Målet med studien är att via fältarbete, geokemisk och optisk analys, undersöka de rumsliga variationerna av K, U och Th – samt undersöka i vilka mineral U och Th finns. Studiens huvudfokus var att diskutera den möjliga utsträckningen för Sahlgrenska-anomalin, tecken på möjliga hydrotermala och tektoniska händelser i området. Den rumsliga variationen av Th visar lokalt förhöjda halter vid Sahlgrenska-anomalin samt ökande koncentrationer i väst. U har låga halter runt Sahlgrenska-anomalin. Kalium visar förhöjda halter runt Sahlgrenska-anomalin, men har normala halter för granit i resten av studieområdet. Studien har visat nya normalvärden för radioaktiva ämnen, 3.5-5 % K, 7-18 ppm U och 30-70 ppm Th. De radioaktiva grundämnena U och Th hittades i de accessoriska mineralen zirkon och titanit, både primärt kristalliserade och möjligen även sekundärt kristalliserad titanit. Ingen biotit upptäcktes, men istället fanns det typiskt hydrotermala mineralet klorit, så all biotit kan ha blivit omvandlad till klorit. Allanit upptäcktes i tidigare studier, men inte i denna. U/Th-ratiorna indikerar hydrotermal omvandling både i delar av Änggårdsbergen men också runt Sahlgrenska-anomalin. Sammanfattningsvis så har vi nya normalvärden för RA-graniten, det har skett hydrotermal omvandling i Sahlgrenska-anomalin och tektoniska händelser speglas i den mikroskopiska analysen.

**Nyckelord:** *RA-granit, uran, kalium, torium, hydrotermal omvandling, Änggårdsbergen, Göteborg, zirkon*

## Table of Contents

# 1. Introduction

## 1.1 Background and aim

Änggårdsbergen in Gothenburg and its surroundings is an interesting site for studying the amount of radioactive elements in the bedrock. It has been measured before with airplane by Sveriges Geologiska Undersökning (SGU) and also with gamma-ray spectrometry in recent bachelor theses in geology from the University of Gothenburg. Among the main result of these studies have been that high contents of Uranium (U) and Thorium (Th) have been found in primary accessory minerals in the RA-granite (also known as Kärra Granit), which is the dominating rock type of Änggårdsbergen. In previous bachelor thesis the Sahlgrenska anomaly (sample 16FF200) was distinguished with higher concentrations of Th and Potassium (K) than the rest of the area of Änggårdsbergen (Hultin & Håkansson, 2018). According to previous bachelor thesis (Hultin & Håkansson, 2018; Cooper Svensson & Lundin Frisk, 2018) U and Th sits in the primary accessory minerals monazite, zircon and allanite and there was an increase in Th-concentrations in Änggårdsbergen from east to west. The ratio of U/Th in the sample 16FF200 was lower than the normal ratio in granite (0.25) and this was seen as an indication of hydrothermal alteration.

The aim of this study is to map the spatial distribution of U, Th and K concentrations, mainly in the RA-granite in north western Änggårdsbergen, but also around Sahlgrenska University Hospital and Medicinareberget, where the Sahlgrenska anomaly can be found. Spatial distribution of these will be combined with previous years studies in order to obtain the full picture of radioactive concentrations from RA- granite in the field area. Analysis via chemical and optical methods will be made only in the RA-granite, to analyze its petrology and mineralogy. This will be further discussed with three main focuses as seen in the next paragraph.

- Is the Sahlgrenska anomaly isolated?
- Discuss evidence of possible hydrothermal alteration in the field area, close to the Sahlgrenska anomaly.
- Investigate if it is possible to connect the results from the Sahlgrenska anomaly and Medicinareberget to a tectonic event.

## 1.2 Geologic background

The Sveconorwegian province consists of the south western part of Sweden and southern Norway with rocks formed during the 1800 to 900 Ma period. The province is divided into five different segments. These five segments are all dominated by granites and gneiss. From east to west the segments of the province are: the eastern segment, Idefjorden Terrane (the median and western segment), Bamble Terrane, Kongsberg Terrane and the Telemarkia Terrane (Lundqvist et al., 2011).

Gothenburg is situated in the western gneiss segment of the province, the Idefjorden Terrane (see figure 1). In the Gothenburg area there are two bedrock suites (A and B series) consisting of dark mica rich tonalites to reddish granites. A mylonite zone constitutes the border to the eastern gneiss segment, where intense shearing has deformed the bedrock. The western gneiss segment has been metamorphosed several times (Lundqvist et al., 2011). The area has been deformed and affected by melting during the

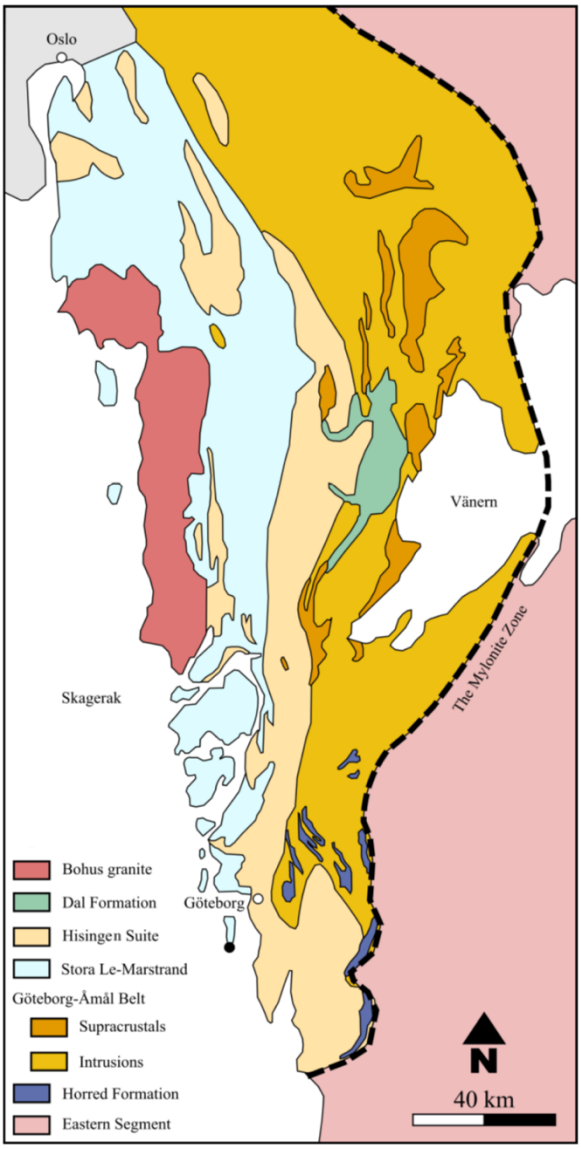


*Figure 1. The Idefjorden Terrane, modified from Åhäll and Connelly (2008) by Eric Ackevall.*

Gothian orogeny followed by the Sveconorwegian orogeny. During the Gothian orogeny, 1650-1500 Ma, several generations of granitoids intruded a large amount of the earlier formed bedrock. During the Sveconorwegian orogeny, 1150-900 Ma, the area was deformed, folded and metamorphosed (Lundqvist et al., 2011). Both orogenesis have given the bedrock a gneiss structure and some bedrock were affected by partial melting creating red to white quartz feldspathic rich veins, the so called Ådergnejs. Intense magmatic activity took place in the time between the Gothian and Sveconorwegian orogeny and this was when the Kungsbacka bimodal suite intruded (Austin Hegardt et al., 2007).
The period after the Sveconorwegian orogenesis is marked by extension and intrusion. The intrusions cut their way over the deformations from the Sveconorwegian orogeny. Many of the intrusions are pegmatite or undeformed granites such as the Bohus granite. Pegmatite intrusions older than the Bohus granite can be found such as one in Änggårdsbergen with beryl, which is dated to 1030 Ma (Lundqvist et al., 2011).

In this study the main focus is RA-granite. RA stands for radioactive as this granite has anomalous high contents of U and Th (Lundqvist et al., 2011). It is also referred to as Kärra granite and is one of three granites associated with the Kungsbacka bimodal suite intrusion. The Kungsbacka bimodal suite is a magmatic suite in north-south direction between Trollhättan in the north to Kungsbacka in the south (Austin Hegardt et al., 2007). The RA-granite is situated along the Göta Älv shear zone. On the east side of the RA-granite is the Gothenburg suite (A-serie) and on the west side the Hisingen suite (B-serie), which are part of the Idefjord terrane (the western segment) (Lundqvist et al., 2011).

The RA-granite is an intrusive granite from mid-proterozoikum, dated to 1325±8 to1311±8 Ma. The dating has been made based on U-Pb concentrations found in zircons (Austin Hegardt et al., 2007). It is spread out in a north south direction and has only been deformed by the latest orogeny. It is red-grey to red in color and contains the main minerals K-feldspar, plagioclase, quartz and biotite with common accessory minerals such as zircon and titanite. In some parts the granite is folded, veined and with K-feldspar augen. Previous bachelor theses have shown that the RA-granite in Änggårdsbergen is peraluminous (having higher proportion of aluminium oxide than the combined sodium oxide, potassium oxide and

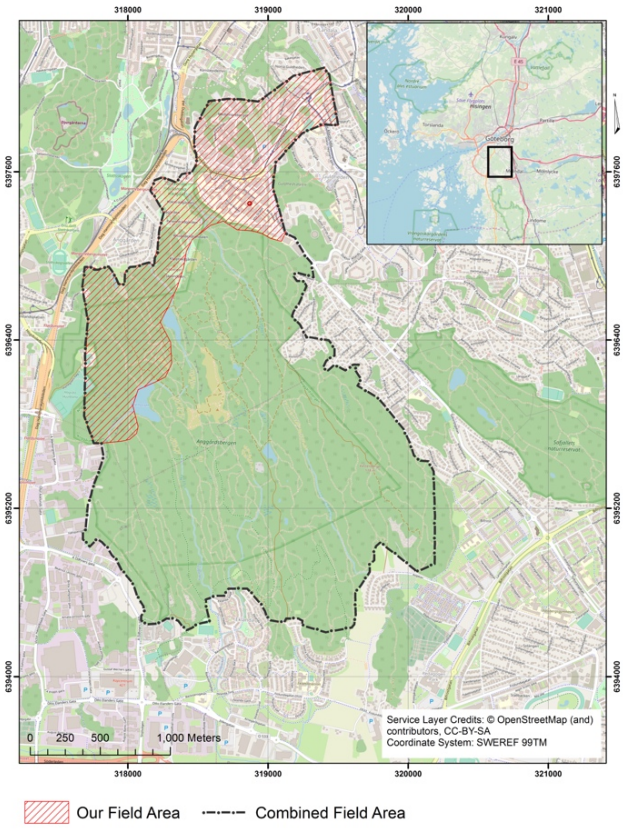


*Figure 2. Overview of our study area, Änggårdsbergen, Medicinareberget and Sahlgrenska University Hospital together with the area from previous bachelor theses. The focus area of the 2019 study, the small one, is about 3.1 km long and 0.7 km wide.*

calcium oxide) and is most similar to the anorogenic (A-type) granite composition (Cooper Svensson & Lundin Frisk, 2018). The A-type granite is often related to continental rift events, and Kungsbacka bimodal suite intruded under such conditions (Austin Hegardt et al., 2007.

## 1.3 Field area

The area of interest for this thesis is situated in the north west part of Änggårdsbergen/Gothenburg Botanical Garden, in the vicinity of the Sahlgrenska University Hospital and Medicinareberget where the Sahlgrenska anomaly is situated. Änggårdsbergen, the Gothenburg Botanical Garden and Sahlgrenska University Hospital/Medicinareberget is located 3 km south of the Gothenburg city center and 5 km in the eastern direction from Mölndal. The field area is a part of the Idefjord Terrane (the western segment), west of the Göta Älv zone. As seen in figure 2, the red area is the area of interest for this thesis, but conclusions and results will be combined with the larger field area from previous bachelor theses.

Änggårdsbergen is a protected nature reserve situated between Gothenburg and Mölndal in Västra Götaland County (see figure 3). Änggårdsbergen covers 352 hectares (Länsstyrelsen, n.d.) and is dominated by RA-granite. Parts of southern Änggårdsbergen have heavy gravel-weathered granite. There are also areas consisted of gneiss with intrusions of amphibolite (Aspfors, 1999). A fracture zone exists at the eastern border of the RA-granite towards a nearby older gneiss. The zone is characterized by a valley from Mölndal to Gothenburg via Toltorpsdalen with few fracture areas in the same direction as Toltorpsdalen.

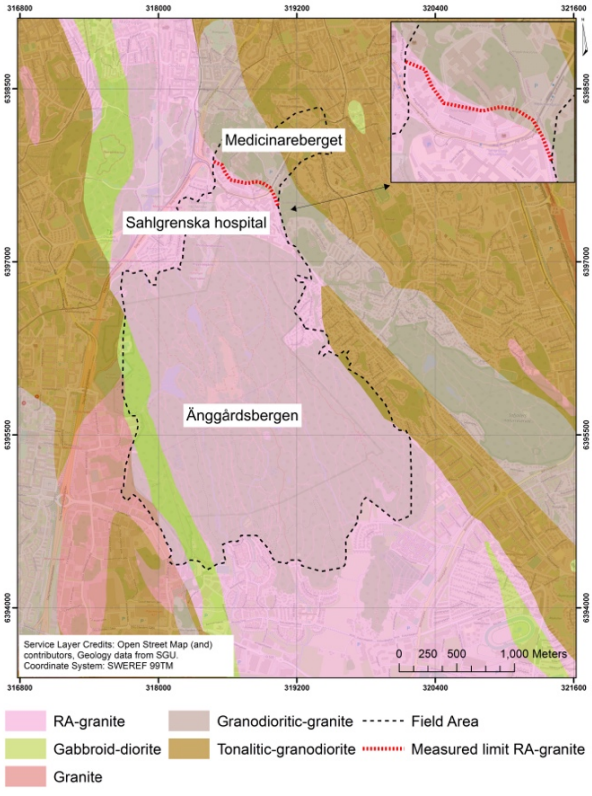


*Figure 2. Overview of the bedrock around Änggårdsbergen, Sahlgrenska University Hospital and Medicinareberget. See appendix B for the measured border of the RA-granite.*

The topography of Änggårdsbergen consists of granitic ridges with fracture valleys, filled with vegetation and soil (Länsstyrelsen, n.d.).
The Sahlgrenska University Hospital area consists of large municipality buildings with few bedrock outcrops mainly consisting of RA-granite. At Medicinareberget there are some RA-granite but mainly metamorphic granitoids with pegmatite intrusions and a few amphibolite intrusions. Some parts of the granitoid are augen bearing.

## 1.4 Radioactivity in rocks

The radioactive elements in a mineral control the radioactivity of the rock. Among the common radioactive elements in minerals are U, Th and K which are also the only ones that gives a detectable signal to a gamma ray spectrometer. Alpha, beta and gamma rays are the three types of radiation. Relevant for our study are the gamma rays since alpha and beta rays weaken too fast to be detectable (Musset & Khan, 2000). The concentrations of U, Th and K vary greatly depending on rock type. The normal concentrations in RA-granite according to SGU can be seen in table 1. However, these concentrations have been measured from airplanes and in a previous study from Bohus-Malmön, airplane measurements showed generally lower values than the hand-held gamma spectrometer (Johansson, 2014). Previous bachelor theses have presented that U and Th resides in the primary accessory minerals monazite, zircon and allanite in the RA-granite. The values from SGU can be compared to values from the sample 16FF200 previously collected at the Sahlgrenska anomaly which showed a thorium concentration of 100 and 200 ppm respectively when measured by a gamma spectrometer and geochemically analysed (Hultin & Håkansson, 2018).

*Table 1. Normal values of some radioactive elements in RA-granite. Airborne measurements by SGU, 2015.*

| Element | Concentration |
|---|---|
| Potassium (K) | 4-6 % |
| Uranium (U) | 8-40 ppm |
| Thorium (Th) | 10-90 ppm |

## 1.5 Hydrothermal alteration

Hydrothermal alteration are processes influenced by e.g. a heated hydrous flow along grain boundaries. These processes help rock-forming minerals to alter due to the reactions following a hydrothermal effect. Hydrothermal activity in the past could be found due to minerals that result from hydrothermal alteration (Berger, 1998). Ion exchange, recrystallization, dissolution and precipitation can create mineral alteration. The contributing physical factors on mineral alterations are pressure, the fluid's chemical composition, temperature and the chemical properties of the wall rock (Berger, 1998). In temperatures higher than 300°C hydrothermal alteration of quartz and feldspathic rocks may create epidote, chlorite and mica. The quartz content may also be altered (Bruhn et al., 1994).

During oxidizing conditions uranium will form water soluble compounds and is easily leached. Hydrothermal alteration on the minerals therefore makes the U/Th ratio smaller (Musset & Khan, 2000). But in reducing condition Uranium and Thorium are chemically similar in the magma and retains the normal U/Th ratio value of granite, 0.25 (Musset & Khan, 2000). In the 2018 bachelor theses the value of U/Th ratio in the sample collected at the Sahlgrenska anomaly was 0.096. This was found to be a result of hydrothermal alteration (Hultin & Håkansson, 2018). The mean value of the U/Th ratio in RA-granite in Änggårdsbergen based on previous bachelor theses is 0.27, which is considered a normal value.

# 2. Method

## 2.1 Field work

The field work area was divided in two sections, see figure 4. The first section was the area around the Sahlgrenska University Hospital/Medicinareberget and the second section was the area in Änggårdsbergen/Gothenburg Botanical Garden. The choice of the area in northern Änggårdsbergen was based on the need for better spatial resolution of U-, Th- and K-concentrations. The area surrounding Sahlgrenska University Hospital and Medicinareberget was chosen with the perspective of better spatial resolution and in order to find the possible extension of the anomaly.

During the fieldwork rock samples were collected and gamma spectrometry was performed. Both of these methods depend upon good sampling sites. Gamma spectrometry measurements were made in RA-granite and surrounding rock types, to see the extension of the anomaly. Rock samples were collected only in RA-granite (see figure 5), close to the Sahlgrenska anomaly, to get a better understanding of the RA-granite and what might cause an anomaly. The rock samples were later sent for geochemical analysis and thin section production, see table 2.

Rock sample collection choice was based upon the degree of weathering, joints and joint fill. The less of these, the better sample for further analysis. The Sahlgrenska University Hospital/Medicinareberget area being in a hospital area means it has a lot of buildings and vegetation which makes it hard to find visible bedrock. The hospital is built on flat ground on a clay filled valley. The visible bedrock was also weathered with a lot of joints, which had to be taken into notice when collecting samples.

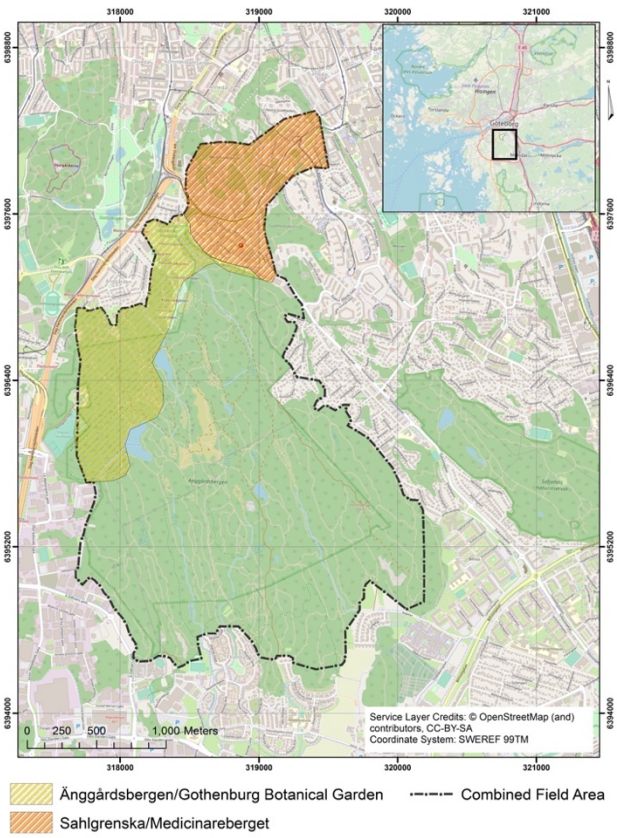


*Figure 3. The two sections of the field area studied 2019.*

Gamma spectrometry measurements were made in Änggårdsbergen, Sahlgrenska University Hospital and Medicinareberget in order to measure the concentrations of U, Th and K. When choosing the spot for measurements a few criterias were used. The spot had to be clean from vegetation in a ca 50 cm radius and it also had to be flat, with at most a few degrees of slope. When collecting data, the bedrock had to be dry, with little to no moisture covering the site. If the bedrock would be wet a slight measuring error would exist which would make the result inaccurate.

In order to know the quality of the measurements a 0-3 scale assessment was made on each site based on information from Thomas Eliasson, SGU. Scale 0 is an unmeasurable site and scale 3 is an excellent site.

*Table 2. A list of rock samples taken for this study.*

| Sample ID | Lon. | Lat. | Sample type |
|---|---|---|---|
| 19FJ001 | 11.956104 | 57.683398 | Geochemical analysis and microscopy |
| 19FJ006 | 11.962900 | 57.684397 | Geochemical analysis and microscopy |
| 19FJ055 | 11.968541 | 57.673720 | Geochemical analysis |
| 19FJ056 | 11.957613 | 57.684009 | Geochemical analysis |

In connection with the gamma spectrometry measurements, structures of the bedrock, visible mineral composition and color were noted. Strike and dip measurements were made on fractures and foliations if possible. On 45 different sites, 20 susceptibility measurements at each site were made. These measurements were made with a Susceptibility Meter JH-8 and the result was noted in order to see if there might be a correlation between magnetic susceptibility and Th-concentrations (see appendix C).

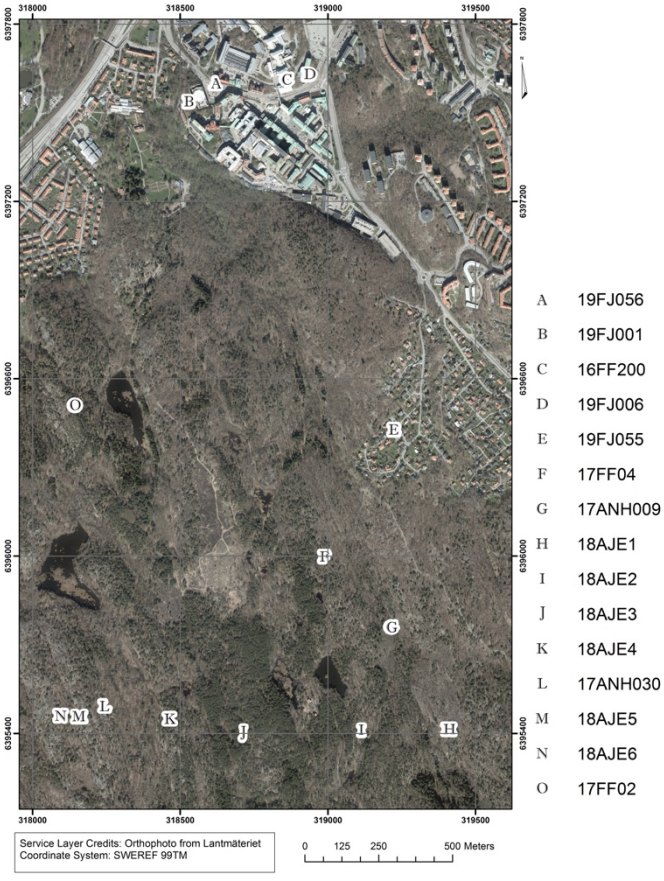


*Figure 5. Visualization of all the rock samples collected for the study of Änggårdsbergen, Medicinareberget and the Sahlgrenska University Hospital area. The year the sample is collected is indicated in the beginning of the sample name.*

Fifty-six sites were measured with a gamma spectrometer based on the criterias mentioned above (see figure 6 and appendix C). Each measurement lasted for 180 seconds and three measurements per area was made in a triangular shape, to prevent very local anomalies to dominate the result (nugget effect). A mean value for each element concentration was calculated. Each measurement site was noted with a GPS with longitude and latitude in EPSG 4326:WGS 1984 and compiled into an Excel document prepared for use in the software ArcMap. In order to distinguish the Sahlgrenska anomaly, measurements were made surrounding it and based on these a border was later interpolated in ArcMap. Additional gamma spectrometry data was provided by Prof. Erik Sturkell, mainly to interpret the area surrounding the Sahlgrenska anomaly.

The gamma ray spectrometer used was of the model RS-230. Its detecting part consists of a Bismuth Germanate crystal with which the gamma ray photons interact and generates a light pulse. The light photon then strikes the photocathode in the following part of the instrument and causes the photocathode to emit a photoelectron. The photoelectron gets amplified into a detectable signal which then is measured. The frequency of the signal of a specific amplitude is then counted, and the frequency is compared to

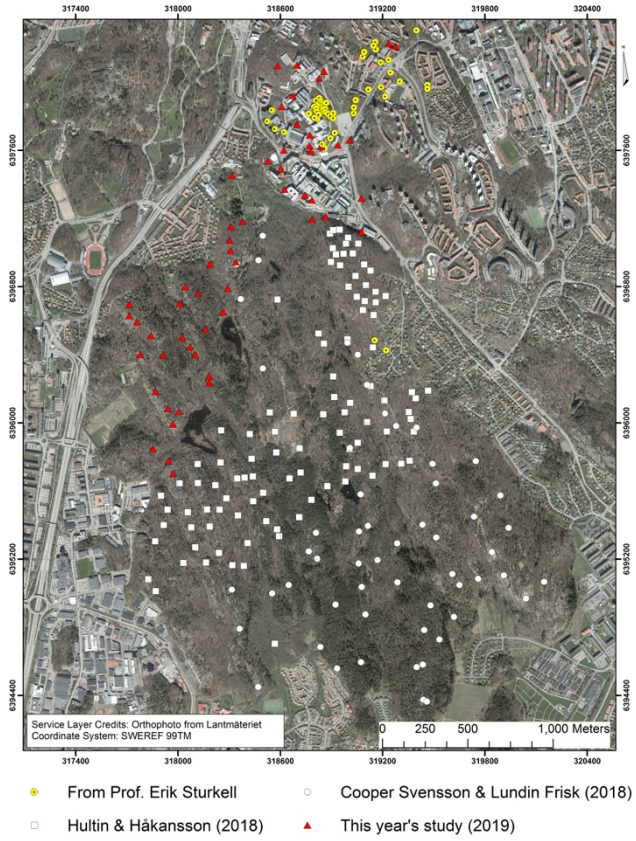


*Figure 6. Visualization of all the sites where gamma spectrometry was done for this study, together with data from two previous bachelor theses.*

that of different elements. Thus the concentrations of elements is calculated.

## 2.2 Laboratory

Four samples from RA-granite were prepared for geochemical analysis and two for thin section production. Rock samples 19FJ001, 19FJ006, 19FJ055 and 19FJ056 were cleaned, sawed to proper size and sent to the ALS Chemlab laboratory in Öjebyn, Piteå. The analysis program used is called the ME-ICP06 CCP-PKG01, Whole Rock Package ICP-AES. The aim with this analysis was to obtain information about the concentrations of chemical elements in the rock.

In order to confirm if the samples show a peraluminous composition this formula was used based on the result from the laboratory samples:

$$\frac{Al_2O_3}{K_2O + Na_2O + CaO} > 1$$

An index value greater than one shows a peraluminous composition (Best, 2003).

Concentrations of Rare Earth Elements (REE's) were normalized towards chondrite values and compared with previous year's rock samples taken in Änggårdsbergen in order to obtain a result for the RA-granite as a whole.

## 2.3 Microscopy

The samples for thin sections, 19FJ001 and 19FJ006, were prepared by sawing to a proper size at the sawing laboratory of the University of Gothenburg, packed and sent to Thin Section Laboratory in Toul, France. The thin sections were prepared in Toul and sent back to the University where they were used in microscopy studies.

The samples 19FJ001 and 19FJ006 together with samples from previous bachelor theses provided by Prof. Erik Sturkell was studied in the Microscopy laboratory belonging to the University of Gothenburg. Previous year's thin sections will not be discussed in this thesis except for 16FF200, also called the Sahlgrenska anomaly. It has been thoroughly studied in previous theses and will be used as a comparison in our discussion.

Minerals were identified for each thin section. The shape of the minerals, relationships between the different minerals but also optical properties were noted and analysed. Pictures of the most interesting minerals were taken in both plane light and cross-polarized light.

This was followed by more advanced analysis in a Scanning Electron Microscope (SEM), with the purpose of identifying which minerals hosted the radioactive elements but also to confirm the minerals seen in the Leica DM RXP microscope. Minerals indicating hydrothermal effect on the rocks were noted and will be further presented in the result and discussion.
When using the SEM-microscope the thin sections had to be prepared with a carbon layer to prevent electron buildup. The carbon layer was applied in a BAL-TEC CED 030 Carbon Evaporator. The SEM-microscope model used was a Hitachi S-3400N Scanning Electron Microscope. The thin sections were looked at in the SEM-microscope with BSE using a working distance of 9.1-9.9 mm and with an acceleration voltage of 20 kV. The microscope was calibrated against cobalt standards to get correct concentrations. The spectrum values were analyzed with the software Inca platform created by Oxford Instruments. This was done to obtain concentrations of elements in chosen local areas in the thin sections to identify minerals but also identifying in what minerals U and Th resided in the thin sections.

## 2.4 Data processing and visualization

For presenting pictures and conducting visual analysis in the report ArcMAP version 10.6 and ArcGIS Pro version 2.3 were used. The presented GPS coordinates for sample points were first in the coordinate system EPSG:4326 (WGS 84) and were then transformed for the use in ArcGIS to EPSG:3006 (SWEREF 99TM).

The data of both gamma spectrometry and rock samples were added to ArcMap with the purpose of creating interpolation maps of the radioactive elements and visualize the sample points. Together with gamma spectrometry results from Hultin and Håkansson (2018), Cooper Svensson and Lundin Frisk (2018) and results provided by Professor Erik Sturkell, radiometric maps were created.

When presenting the radiometric values, the Inverse Distance Weighting (IDW) interpolation method in ArcMap was chosen. Default settings were used with the field area polyline as a mask. The IDW maps were split into two for each element: one for RA-granite and one for the area with no RA-granite. A few sample points were removed (see appendix C) from Änggårdsbergen where there were no RA-granite. During symbology classification in ArcMap, a stretched classification was used based on maximum and minimum values.

The susceptibility result was also presented in an IDW map, combined with previous year's results. The median value of the 20 measurements on each site was used. Previous years had used different ways to present the data (median or mean) so this had to be taken into note when presenting the maps. Default settings for IDW were used but with a mask of a polyline covering the area. A symbology classification with a stretched classification (maximum and minimum values) was made in order to show the distribution of the susceptibility over the field area.

Histograms and graphs were created in Microsoft Excel Version 15.34 for the concentrations of radioactive elements and were made only with the RA-granite in Änggårdsbergen. Together with data from Bohus-Malmön (Bohus granite), an area around Geovetarcentrum (department of Earth Sciences at the University of Gothenburg) with a low-radioactive rock type (granodiorite/tonalite), and data from the Stigfjord granite, a graph was created with the aim to see differences between the rock types.

# 3. Result

## 3.1 Gamma spectrometry

### 3.1.1 Potassium (K)

The concentrations of K are between 2.27 % and 9.8 % with a mean value of 4.31 % in the RA-granite. Around the Sahlgrenska anomaly (seen in the magnification in figure 7) there is an area with higher concentrations of K.
A few other high values are strewn in Änggårdsbergen, but they are isolated. The area has generally quite low concentrations of K.

In the granodiorite/tonalite at Medicinareberget and its vicinity there are generally low concentrations of K, with a few higher values in the western part of the area.

When combining all data of RA-granite (including previous bachelor theses) in Änggårdsbergen alone, the histogram indicates that most of the K ranges between 3.5-5 % (see figure 7C) and shows quite a normal distribution.

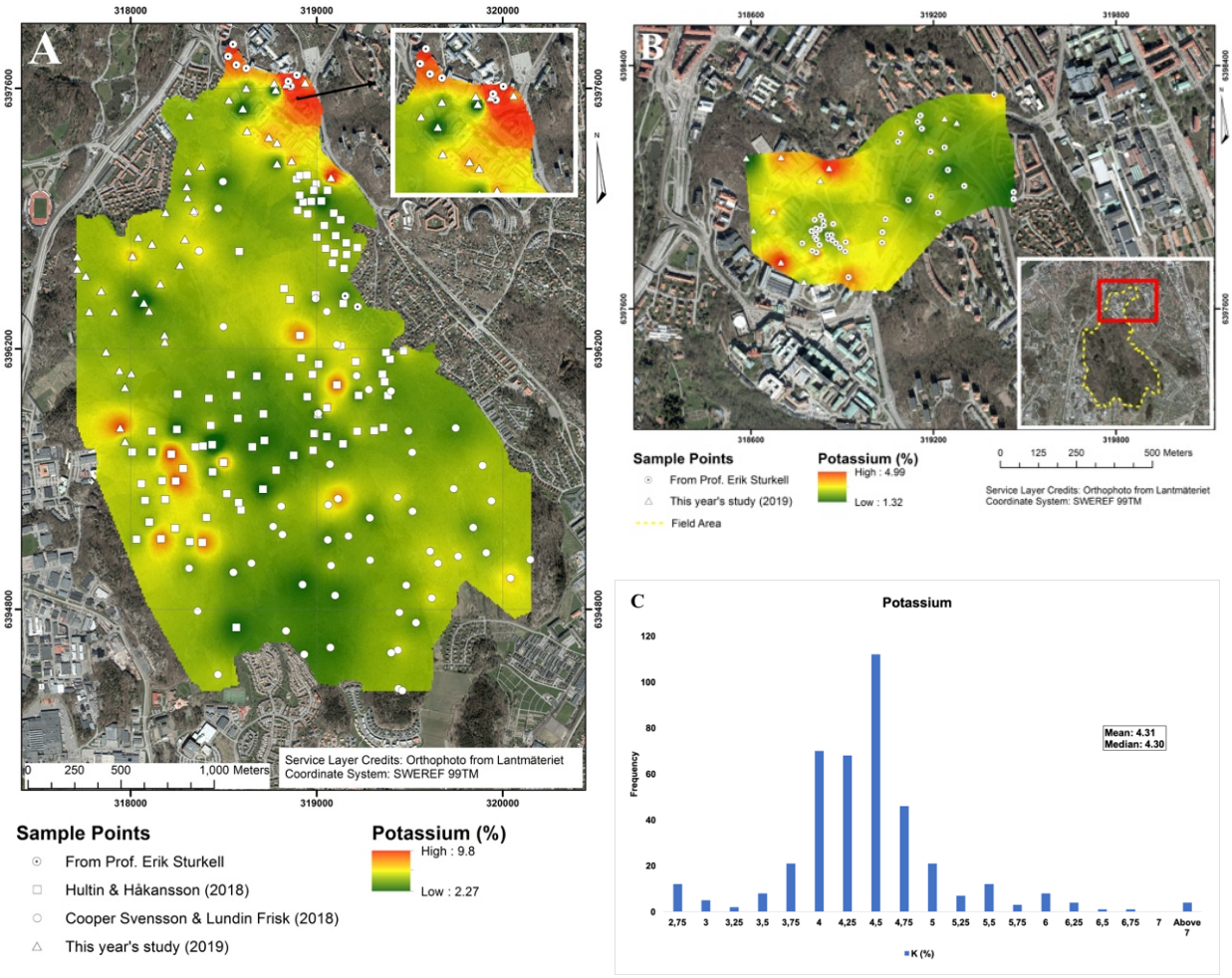


*Figure 7. Gamma spectrometry measurement of K. A) Interpolation map for K-concentrations in RA-granite (Änggårdsbergen and Sahlgrenska University Hospital). B) Interpolation map for K-concentrations at and around Medicinareberget (granodiorite and tonalite). C) Histogram of the K-concentrations plus mean and median for all the data from Änggårdsbergen.*

### 3.1.2 Uranium (U)

The concentrations of U are between 4.78 ppm and 40.79 ppm with a mean value of 12.33 ppm in the RA-granite. There is one sign of higher concentrations around the Sahlgrenska anomaly, but it is a bit to the west, see figure 8. One area in the south and one in the northwest of Änggårdsbergen has high concentrations of U and there is a band of lower concentrations in an approximately north-south direction. The area has generally neither high or low concentrations of U, but something in between.

In the granodiorite/tonalite at Medicinareberget and its vicinity there are generally low concentrations of U, with two higher values in the western part of the area, but they are still low compared to the RA-granite.

When combining all data of RA-granite (including previous bachelor theses) in Änggårdsbergen alone, the histogram indicates that most of the U ranges around 7-18 ppm (see figure 8C) and shows quite a normal distribution.

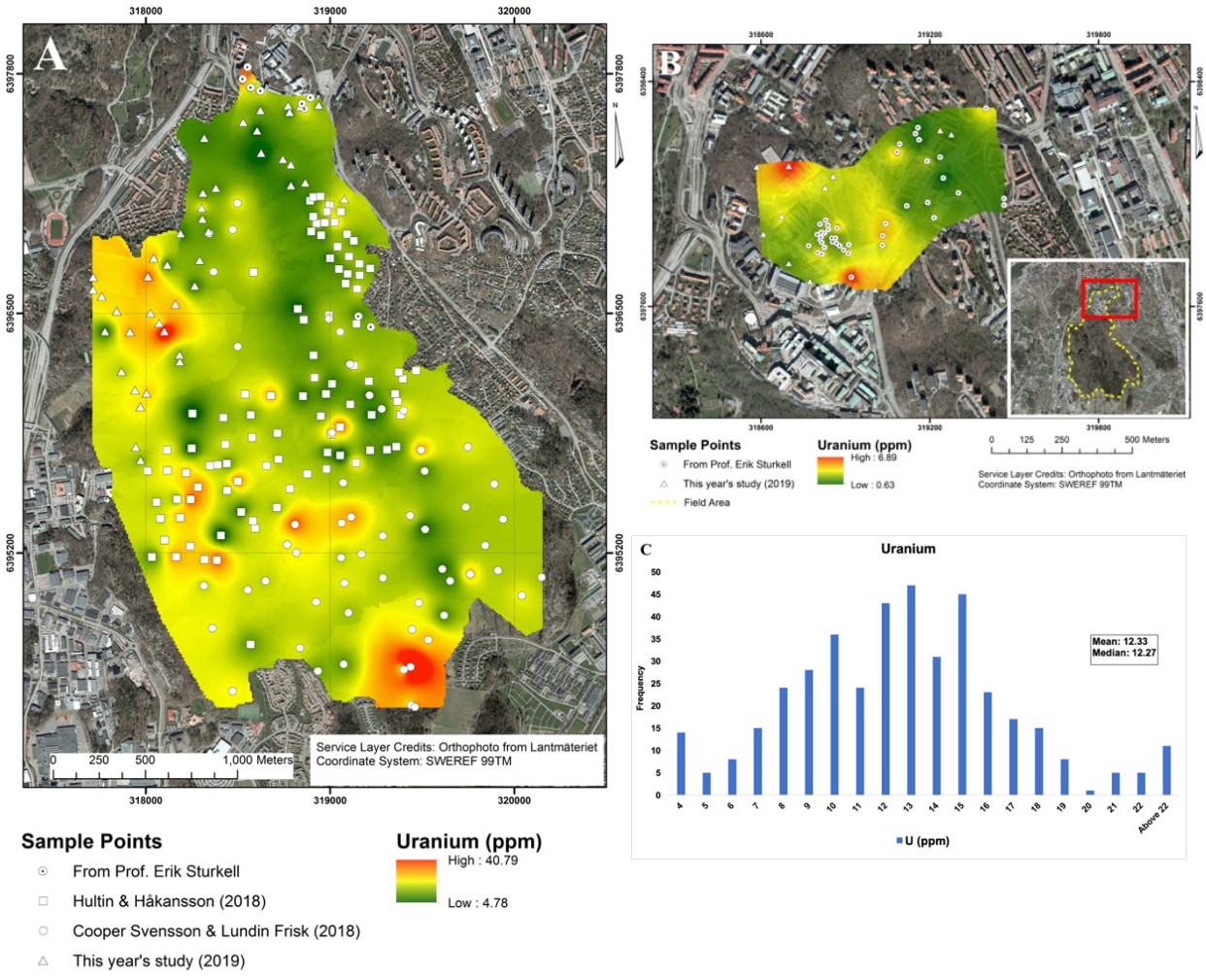


*Figure 8. Gamma spectrometry measurement of U. A) Interpolation map for U-concentrations in RA-granite (Änggårdsbergen and Sahlgrenska University Hospital). B) Interpolation map for U-concentrations at and around Medicinareberget (granodiorite and tonalite). C) Histogram of the U-concentrations plus mean and median for all the data from Änggårdsbergen.*

### 3.1.3 Thorium (Th)

The concentrations of Th are between 14.18 ppm and 122.62 ppm with a mean value of 48.5 ppm in the RA-granite. Around the Sahlgrenska anomaly (seen in the magnification in figure 9) there is an area with higher concentrations of Th, connected with an area to the west. The rest of Änggårdsbergen is divided in two bands going in an approximately north-south direction, the western with higher concentrations and the eastern with lower concentrations.

In the granodiorite/tonalite at Medicinareberget and its vicinity there are generally low concentrations of Th, with one relatively high value in the southern part of the area.

When combining all data of RA-granite (including previous bachelor theses) in Änggårdsbergen alone, the histogram indicates that most of the Th ranges around 30-70 ppm (see figure 9C) and shows a quite good normal distribution.

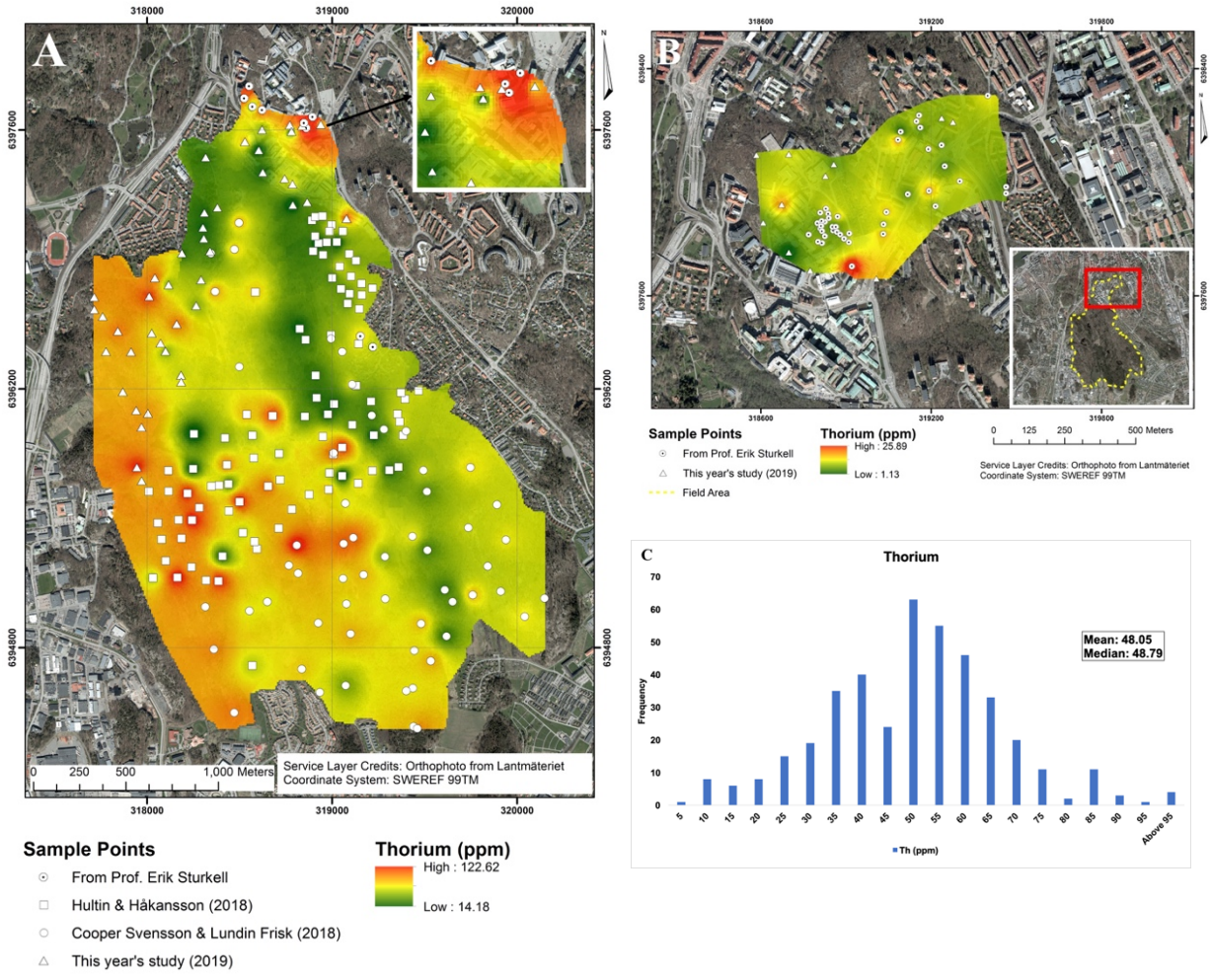


*Figure 9. Gamma spectrometry measurement of Th. A) Interpolation map for Th-concentrations in RA-granite (Änggårdsbergen and Sahlgrenska University Hospital). B) Interpolation map for Th-concentrations at and around Medicinareberget (granodiorite and tonalite). C) Histogram of the Th-concentrations plus mean and median for all the data from Änggårdsbergen.*

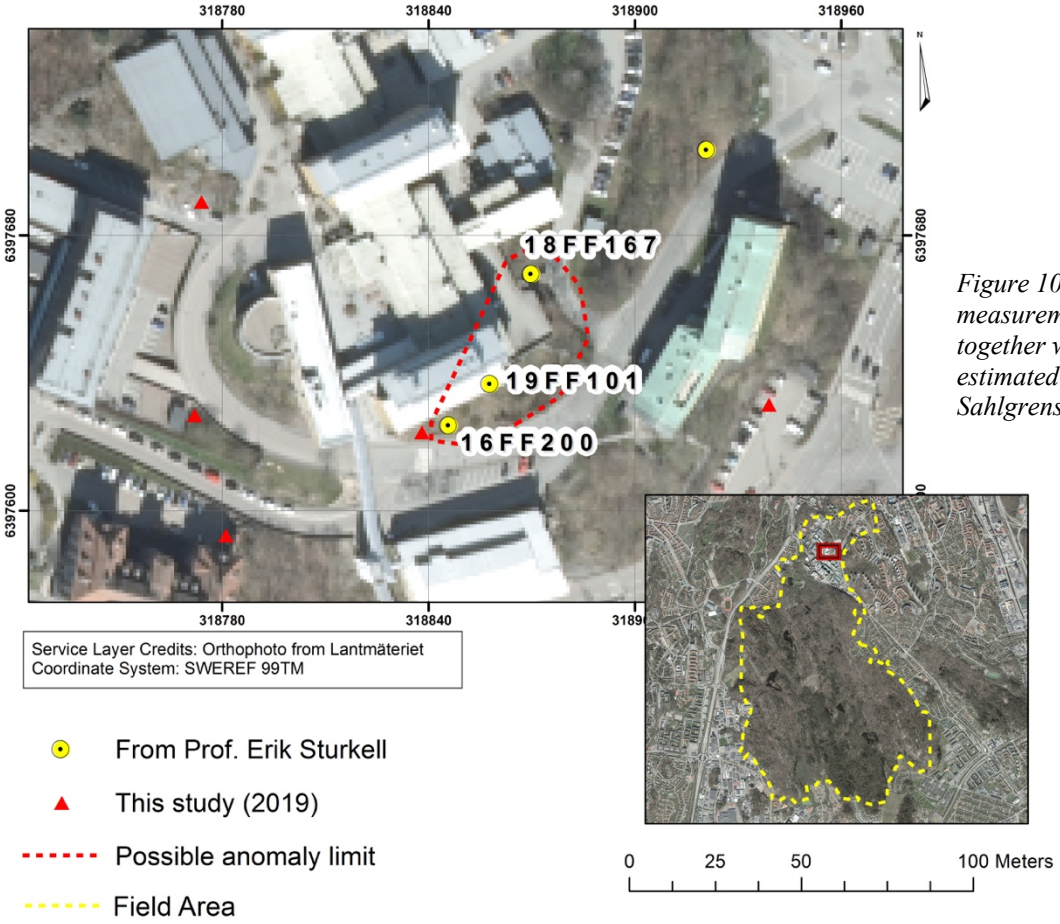


*Figure 10. Gamma measurement sites together with an estimated border of the Sahlgrenska anomaly.*

### 3.1.4 The Sahlgrenska anomaly

Except from the values of the sample 16FF200 there are fairly high values (from the 2019 study) surrounding the Sahlgrenska anomaly with higher concentrations of K and Th than the rest of the nearby area. As seen in figures 7 and 9 the area of higher K- and Th-concentrations are isolated with no widespread concentrations in the higher magnitude. Thorium-concentration values in the vicinity of the anomaly ranges between 25.9-123.16 ppm (not exclusively RA-granite), where the higher values (100 ppm and 123 ppm) consists of just two sample points (16FF200 and 18FF167, 19FF101 has a lower value, 78.6 ppm Th, but is included in the anomaly) close to each other (see figure 10) K-concentrations varies between 2.2 % and 9.8 % (including extra data from Prof. Erik Sturkell).

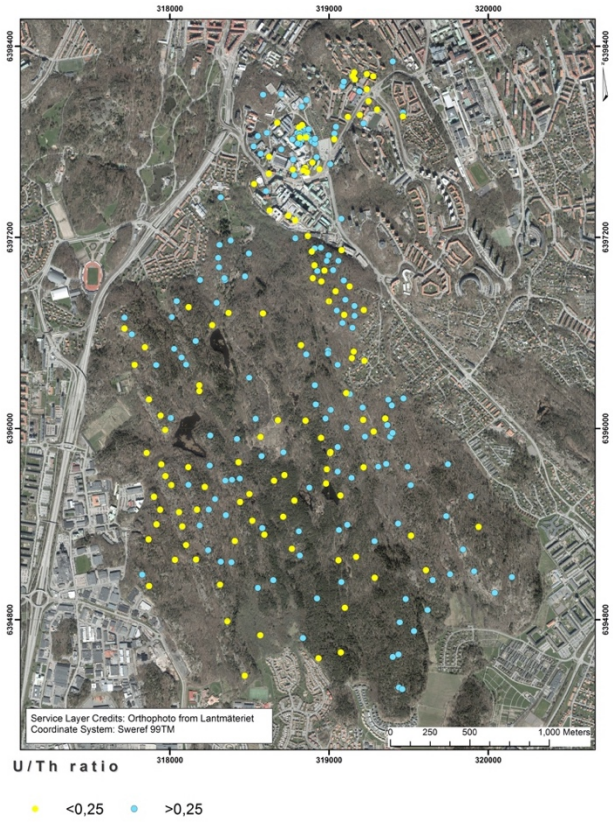


*Figure 11. Map of the U/Th ratios.*

### 3.1.5 U/Th ratios

The mean value of U/Th ratio in the field area of the 2019 study is 0.30. The highest ratio is 1.53 and the lowest value is 0.14. When looking at our result in detail there are 23 out of 56 measurement sites that show a U/Th ratio below 0.25 (see appendix C).

These measured values are well spread across our field area. This pattern can be seen combined with the data from previous years (see figure 11). The two points within the Sahlgrenska anomaly mentioned in section 3.1.4 have low values of U/Th ratios, well below 0.25. Surrounding the Sahlgrenska anomaly the U/Th ratios in RA-granite are below 0.25 as well. Note that the most northern part of the map is not RA-granite but other granitoids.

### 3.1.6 Comparison between RA-granite and other Swedish granites

The RA-granite based on data from Änggårdsbergen has a wide spread of K-concentrations (see figure 12), but the range of Th-concentrations is much wider. Bohus granite from Bohus-Malmön has approximately the same K-concentrations, but it is not as varied. The low-radioactive rock from around Geovetarcentrum (granodiorite/tonalite) has low concentrations of both K and Th. The Stigfjord granite is quite varied in the K-concentrations but has a narrow span of Th-concentrations compared to the RA-granite.

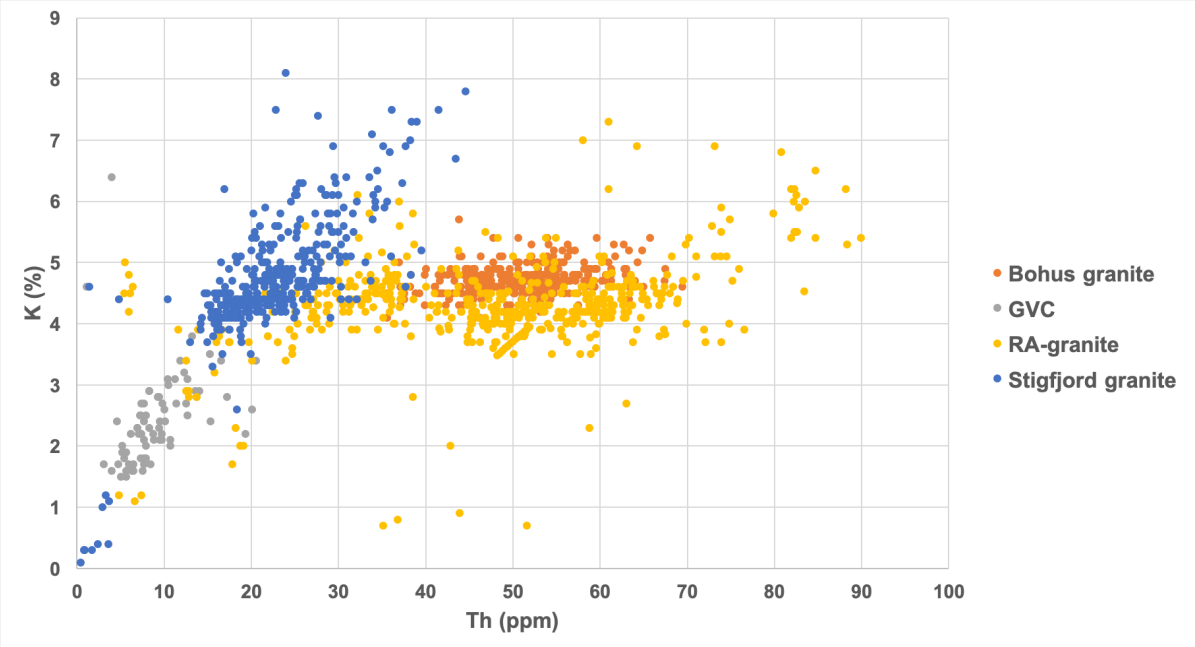


*Figure 12. Comparison of K- and Th-concentrations between RA-granite (not including the Sahlgrenska anomaly) and other Swedish rock types.*

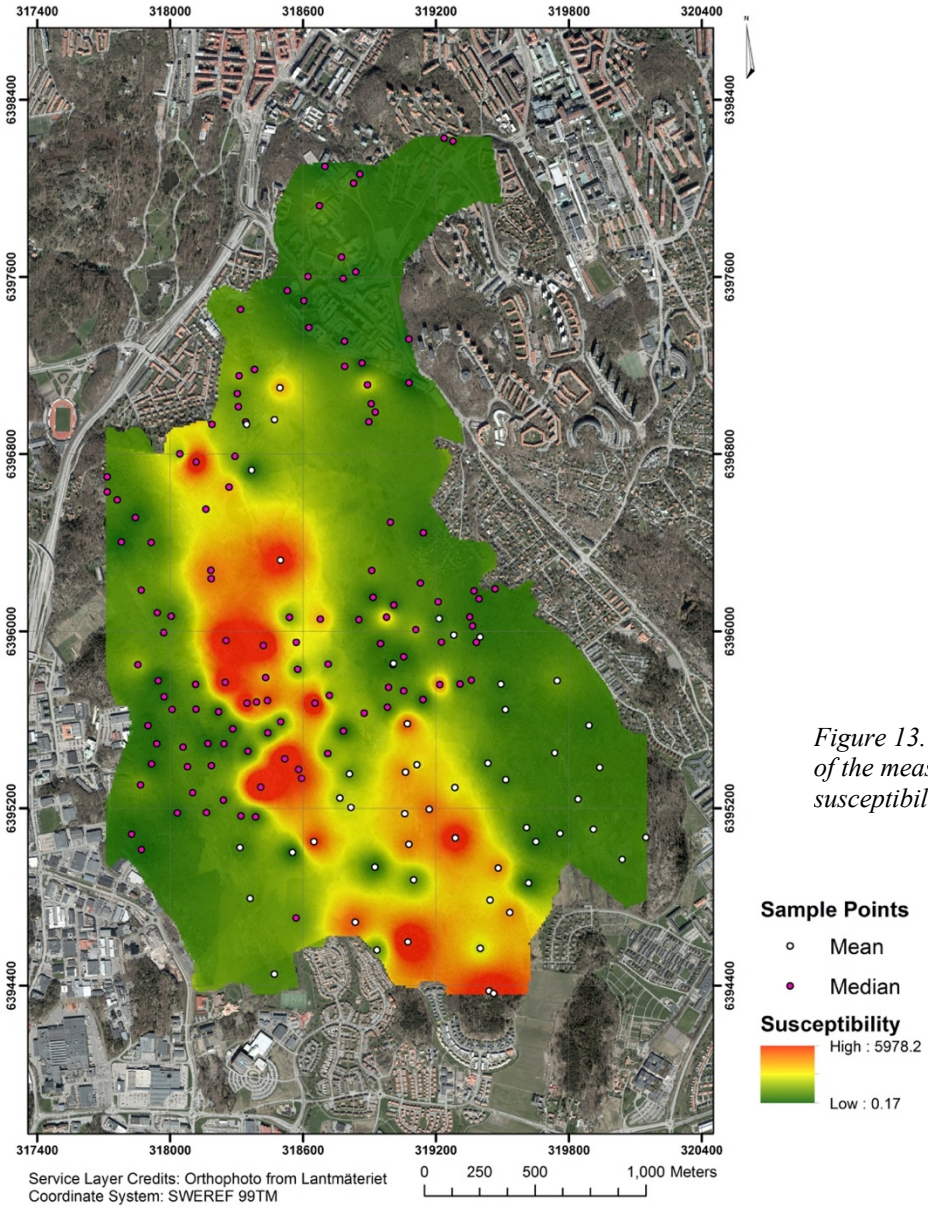


*Figure 13. Interpolation map of the measured magnetic susceptibility.*

## 3.2 Susceptibility

The northern part of the field area is dominated by lower values of susceptibility, and as seen in figure 2 most of this area is not RA-granite. A band with high susceptibility values is seen in the middle of the Änggårdsbergen area (see figure 13), in an approximately north-south direction.

## 3.3 Geochemical analysis

The result from the ALS whole rock chemical analysis (made on 19FJ001, 19FJ006, 19FJ055 and 19FJ056) are presented in table 3 together with the samples from previous studies (16FF200, 17ANH009, 17ANH30, 17FF02, 17FF04, 18AJE1, 18AJE2, 18AJE3, 18AJE4, 18AJE5, 18AJE6). See appendix A for complete element concentrations and see appendix E for sample locations.

The samples are quite alike in the major elements. Sample 16FF200 stands out a bit with two amounts, one higher ($K_2O$), and one lower ($SiO_2$). 19FJ006 are also lower than the others in $SiO_2$. Most of the samples taken in 2018 are low in $Al_2O_3$ (18AJE2, 18AJE3, 18AJE4 and 18AJE6).

The REE's are more varied in the samples. 16FF200 has the highest amount of every single REE by a great deal. 18AJE6 has nearly every time the lowest amount of REE's. 17FF02 and 18AJE2 are quite high in the light REE's while 17FF02 and 19FJ001 are quite high in the heavy REE's.

The samples concentrations of Large Ion Lithophile Elements (LILE) are quite varied. 19FJ006 has high amounts of Sr and Ba. 17ANH009 has generally low concentrations of LILE's.

The High Field Strength Elements (HFSE) are also quite varied. 17FF04 has high amounts of a couple of elements (Nb, Ta, Zr and Hf). 18AJE6 has the lowest amounts of Zr, Hf, U and Y. 16FF200 has the highest amounts of Th, Y and Sc. 19FJ001 has an extremely higher amount of Zr than 19FJ006.

Calculations show that the samples from the 2019 study are peraluminous with index values of 1.41 (19FJ001), 1.46 (19FJ006), 1.37 (19FJ055) and 1.40 (19FJ056). Values from previous years ranged between 1.16 (17FF04) and 1.45 (18AJE1).

Calculations of the U/Th ratio of the samples from 2019 gave ratios of 0.28 (19FJ001), 0.20 (19FJ006), 0.26 (19FJ055) and 0.23 (19FJ056). Concentrations of U and Th are fairly similar in these two samples. Values from previous years ranged between 0.33 (17ANH030) and 0.10 (16FF200 and 18AJE5).

Normalizing the Rare Earth Elements concentrations against chondrite values from Taylor and McLennan (1985) a negative Europium anomaly is visualized (see figure 14). REE values decreases with an increase in atomic number from La to the Europium anomaly. Two samples, 18AJE4 and 18AJE5, have a slightly higher Cerium concentration compared to the REE's.

After Eu the values show no sign of a general decreasing or increasing pattern, instead they align more with each other. 16FF200 has higher concentrations of every element than any other sample.

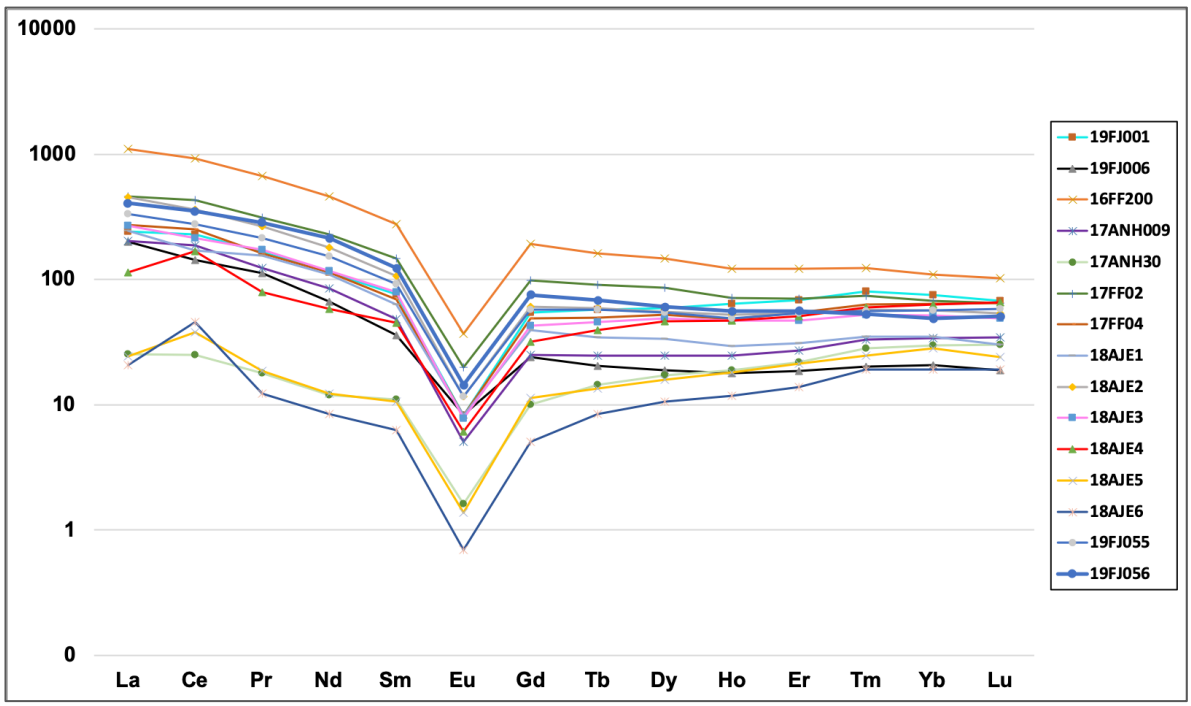


*Figure 14. Chondrite normalized values of REE's for all rock samples from Änggårdsbergen.*

*Table 3. Result from the ALS geochemical analysis program.*

| Elements | Unit | 19FJ001 | 19FJ006 | 19FJ055 | 19FJ056 | 16FF200 | 17ANH009 | 17ANH030 | 17FF02 | 17FF04 | 18AJE1 | 18AJE2 | 18AJE3 | 18AJE4 | 18AJE5 | 18AJE6 |
|---|---|---|---|---|---|---|---|---|---|---|---|---|---|---|---|---|
| **Major elements** | | | | | | | | | | | | | | | | |
| $SiO_2$ | % | 81 | 65.4 | 74.8 | 73.8 | 61.7 | 77 | 77.3 | 74.4 | 76.1 | 75.8 | 73 | 74.5 | 73.3 | 79.5 | 77.7 |
| $Al_2O_3$ | % | 9 | 17.5 | 12.95 | 12.5 | 17.15 | 11.65 | 11.9 | 12.3 | 10.55 | 12.7 | 3.14 | 2.89 | 3.77 | 10.65 | 1.75 |
| $Fe_2O_3$ | % | 4.22 | 2.46 | 2.65 | 4.59 | 5.21 | 1.99 | 1.52 | 4.04 | 4.38 | 2.17 | 3.14 | 2.89 | 3.77 | 1.63 | 1.75 |
| CaO | % | 0.31 | 0.78 | 0.9 | 0.2 | 0.28 | 0.21 | 0.43 | 0.5 | 0.13 | 0.4 | 0.38 | 0.14 | 0.12 | 0.06 | 0.14 |
| MgO | % | 0.22 | 1.29 | 0.2 | 0.04 | 0.6 | 0.24 | 0.22 | 0.02 | 0.03 | 0.28 | 0.31 | 0.02 | 0.03 | 0.24 | 0.18 |
| $Na_2O$ | % | 2.27 | 5.33 | 3.55 | 3.94 | 1.58 | 3.78 | 2.63 | 3.69 | 4.04 | 3.95 | 3.72 | 3.68 | 3.99 | 2.63 | 2.57 |
| $K_2O$ | % | 3.82 | 5.91 | 5.02 | 4.82 | 11.95 | 4.38 | 5.48 | 5.03 | 4.95 | 4.42 | 5.01 | 5 | 5.39 | 4.87 | 5.12 |
| $TiO_2$ | % | 0.21 | 0.38 | 0.22 | 0.37 | 0.49 | 0.23 | 0.22 | 0.36 | 0.3 | 0.22 | 0.33 | 0.27 | 0.31 | 0.22 | 0.2 |
| MnO | % | 0.03 | 0.02 | 0.04 | 0.01 | 0.03 | 0.02 | 0.02 | 0.05 | 0.07 | 0.03 | 0.03 | 0.03 | 0.06 | 0.02 | 0.02 |
| $P_2O_5$ | % | 0.01 | 0.05 | 0.02 | 0.01 | 0.03 | 0.02 | 0.03 | 0.03 | 0.03 | 0.04 | 0.02 | 0.02 | 0.01 | 0.02 | 0.03 |
| $Cr_2O_3$ | % | 0.004 | 0.004 | 0.003 | 0.003 | <0.01 | <0.01 | <0.01 | <0.01 | <0.01 | 0.024 | 0.01 | 0.01 | 0.01 | 0.013 | 0.01 |
| **REE** | | 19FJ001 | 19FJ006 | 19FJ055 | 19FJ056 | 16FF200 | 17ANH009 | 17ANH030 | 17FF02 | 17FF04 | 18AJE1 | 18AJE2 | 18AJE3 | 18AJE4 | 18AJE5 | 18AJE6 |
| La | ppm | 88.2 | 73.1 | 122.5 | 149 | 405 | 74.7 | 9.3 | 169.5 | 99.5 | 89.6 | 166.5 | 98.2 | 41.5 | 8.9 | 7.6 |
| Ce | ppm | 219 | 136 | 20 | 10 | 889 | 180 | 23.9 | 411 | 240 | 162.5 | 344 | 205 | 160.5 | 36.1 | 43.6 |
| Pr | ppm | 22.7 | 15.45 | 29.4 | 38.9 | 91.3 | 16.8 | 2.45 | 42.6 | 22.1 | 21.1 | 36.1 | 23.7 | 10.85 | 2.55 | 1.68 |
| Nd | ppm | 81 | 47.6 | 108.5 | 151.5 | 326 | 60.6 | 8.5 | 162 | 80.4 | 77.4 | 128.5 | 82.8 | 41.2 | 8.7 | 6 |
| Sm | ppm | 17.6 | 8.27 | 21.1 | 28.4 | 63.7 | 11.1 | 2.54 | 34.1 | 15.95 | 14.5 | 24.6 | 18.3 | 10.45 | 2.45 | 1.44 |
| Eu | ppm | 0.71 | 0.72 | 1.01 | 1.25 | 3.19 | 0.44 | 0.14 | 1.73 | 0.71 | 0.71 | 1.01 | 0.68 | 0.53 | 0.12 | 0.06 |
| Gd | ppm | 16.7 | 7.38 | 17.45 | 23.1 | 58.9 | 7.62 | 3.06 | 30.2 | 14.95 | 12.05 | 18.45 | 13 | 9.78 | 3.44 | 1.54 |
| Tb | ppm | 3.32 | 1.18 | 47.9 | 32.9 | 9.36 | 1.42 | 0.84 | 5.26 | 2.87 | 2.01 | 3.41 | 2.64 | 2.28 | 0.78 | 0.49 |

| | | | | | | | | | | | | | | | | |
|---|---|---|---|---|---|---|---|---|---|---|---|---|---|---|---|---|
| **Dy** | **ppm** | **22.5** | **7.19** | **20.6** | **23** | **56.2** | **9.35** | **6.57** | **32.5** | **20** | **12.75** | **20.9** | **18.5** | **17.6** | **6.03** | **4.04** |
| **Ho** | **ppm** | **5.42** | **1.52** | **4.15** | **4.73** | **10.35** | **2.09** | **1.6** | **6.04** | **4.12** | **2.5** | **4.44** | **4** | **3.99** | **1.53** | **1** |
| **Er** | **ppm** | **17.05** | **4.62** | **13.35** | **13.95** | **30.4** | **6.73** | **5.46** | **17.55** | **13.5** | **7.74** | **13.3** | **11.75** | **12.7** | **5.3** | **3.44** |
| **Tm** | **ppm** | **2.88** | **0.73** | **2.01** | **1.9** | **4.46** | **1.19** | **1.01** | **2.66** | **2.28** | **1.26** | **2.08** | **1.88** | **2.16** | **0.89** | **0.69** |
| **Yb** | **ppm** | **18.55** | **5.11** | **14.05** | **12.05** | **27.2** | **8.45** | **7.33** | **16.75** | **15.8** | **8.61** | **14** | **12.75** | **15.6** | **7** | **4.72** |
| **Lu** | **ppm** | **2.57** | **0.72** | **2.21** | **1.93** | **3.86** | **1.31** | **1.14** | **2.45** | **2.45** | **1.14** | **2.05** | **1.86** | **2.48** | **0.91** | **0.73** |
| **LILE** | | **19FJ001** | **19FJ006** | **19FJ055** | **19FJ056** | **16FF200** | **17ANH009** | **17ANH030** | **17FF02** | **17FF04** | **18AJE1** | **18AJE2** | **18AJE3** | **18AJE4** | **18AJE5** | **18AJE6** |
| **Pb** | **ppm** | **20** | **22** | **68** | **9** | **41** | **15** | **29** | **29** | **58** | **44** | **28** | **38** | **41** | **57** | **26** |
| **Sr** | **ppm** | **15.5** | **88.1** | **1** | **<1** | **37** | **36.6** | **23.4** | **24.7** | **2.8** | **27.8** | **19** | **4.5** | **2.4** | **19.2** | **24.8** |
| **Ba** | **ppm** | **41.6** | **479** | **164.5** | **43** | **256** | **133** | **87.5** | **49.3** | **23.1** | **168.5** | **67.3** | **26.4** | **31** | **91.7** | **94.3** |
| **Rb** | **ppm** | **307** | **262** | **454** | **254** | **679** | **204** | **446** | **305** | **548** | **299** | **395** | **448** | **518** | **416** | **363** |
| **Cs** | **ppm** | **1.53** | **2.64** | **4.94** | **2.41** | **4.13** | **0.87** | **9.04** | **1.36** | **4** | **1.3** | **1.3** | **2.18** | **7.98** | **4.23** | **4.41** |
| **HFSE** | | **19FJ001** | **19FJ006** | **19FJ055** | **19FJ056** | **16FF200** | **17ANH009** | **17ANH030** | **17FF02** | **17FF04** | **18AJE1** | **18AJE2** | **18AJE3** | **18AJE4** | **18AJE5** | **18AJE6** |
| **Nb** | **ppm** | **96.4** | **17.4** | **88.3** | **64** | **113.5** | **59.5** | **26.9** | **74.6** | **157.5** | **56.3** | **94.1** | **129** | **123** | **19.6** | **17.9** |
| **Ta** | **ppm** | **6.4** | **1.7** | **5.6** | **2.7** | **10.1** | **3.8** | **2.4** | **5.2** | **11.8** | **4.1** | **6.2** | **6.9** | **8.3** | **2.2** | **2** |
| **W** | **ppm** | **2** | **1** | **2** | **3** | **1** | **1** | **4** | **<1** | **2** | **1** | **2** | **1** | **1** | **<1** | **1** |
| **Zr** | **ppm** | **1600** | **216** | **429** | **1315** | **1625** | **862** | **172** | **1375** | **1865** | **292** | **881** | **1200** | **1210** | **171** | **151** |
| **Hf** | **ppm** | **40.8** | **6.8** | **15.3** | **32.9** | **42.8** | **24** | **7** | **34.8** | **57.3** | **11** | **25.6** | **37.4** | **34.8** | **6.7** | **6** |
| **Th** | **ppm** | **49.9** | **55.4** | **47.9** | **32.9** | **201** | **56.6** | **60.6** | **42.4** | **79.6** | **41** | **55.4** | **66.9** | **63.1** | **77.3** | **63.1** |
| **U** | **ppm** | **14.05** | **10.9** | **12.4** | **7.58** | **19.35** | **9.17** | **19.7** | **10.15** | **14.85** | **12.4** | **11.3** | **13.7** | **10.45** | **7.61** | **7.3** |
| **Y** | **ppm** | **147.5** | **44** | **116** | **120.5** | **306** | **60.3** | **45.3** | **173.5** | **121** | **65** | **125** | **104.5** | **86.2** | **46.1** | **30.2** |
| **Sc** | **ppm** | **<1** | **5** | **1** | **<1** | **5** | **1** | **2** | **1** | **<1** | **1** | **1** | **1** | **1** | **2** | **2** |

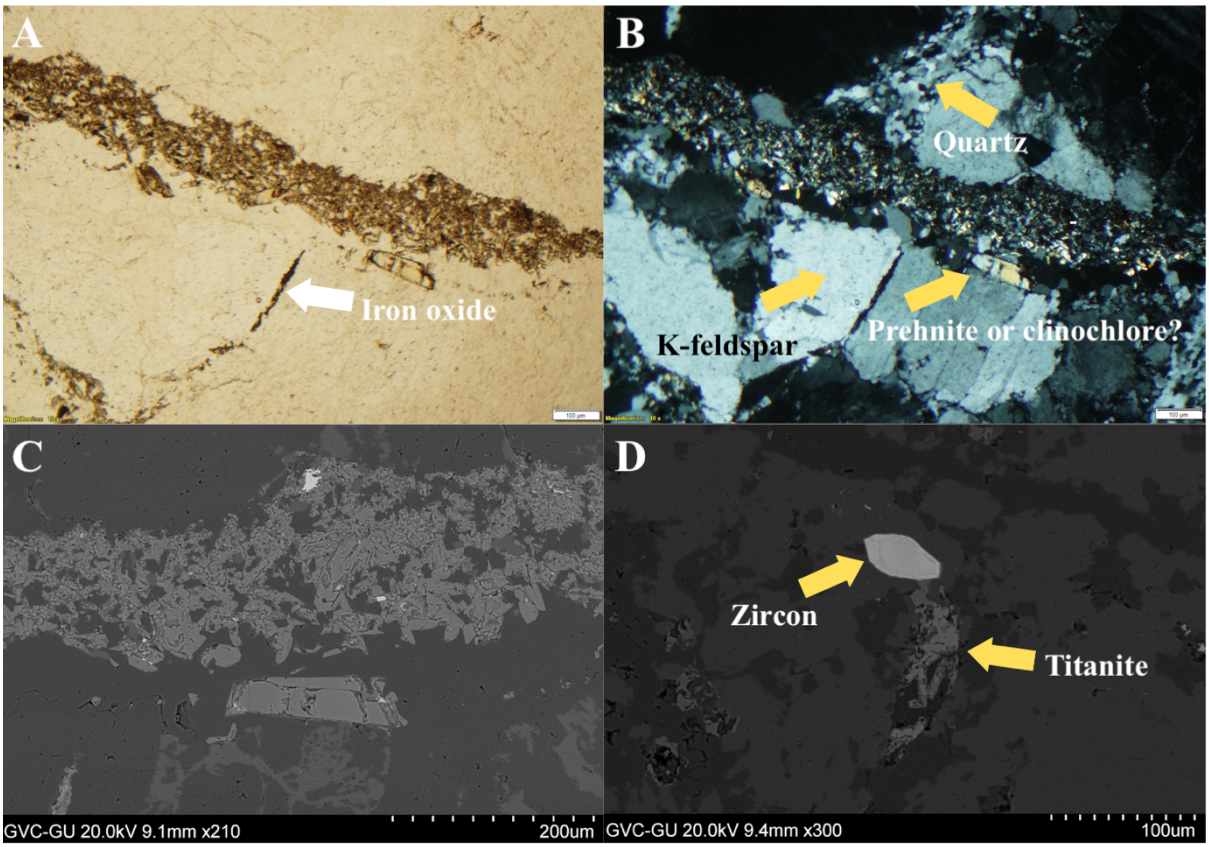


*Figure 14. Pictures of thin section 19FJ001. A) Fracture filled with prehnite or clinochlore surrounded by quartz and K-feldspar. Photo taken in plane light. B) Same as in A, but photo taken in cross-polar light. C) Same as in A and B, photo taken in SEM. D) Titanite and zircon surrounded by K-feldspar and quartz. Photo taken in SEM.*

## 3.4 Microscopy and SEM

### 3.4.1 19FJ001

19FJ001 has wider and smaller fractures, some of which are filled with red/brown iron oxide. The iron oxide also exists as matrix all through the thin section. The fractures are in different directions (see appendix D) and together with the overall appearance of the thin section an influence from different events can be seen to have altered the sample based on presence of hydrothermal minerals, fractures and fracture filling.

19FJ001 shows a high amount of opaques (iron oxides) when analyzing it in a microscope. Many of these have a euhedral or rhombic grain shape. They are probably magnetite and/or hematite and a few of them contain the REE element Ce. Cerium was not exclusive to iron oxides, it was found in other minerals too.

Quartz is the dominating mineral in the thin section, and it is often seen surrounding other mineral grains. The quartz grains of the sample were often small and irregularly shaped. In a few areas quartz is filling fractures. K-Feldspar (microcline) showed tartan twinning (in cross polar light) and fairly large grains could be seen next to plagioclase grains. In a few cases these plagioclase grains had polysynthetic twins, but mostly not.

In the thin section (mostly close to fractures) there are small grains with a high relief and a light brown color in plane light. A yellow/brown/orange color was seen when brought to extinction in cross polar light and this was identified as epidotes.

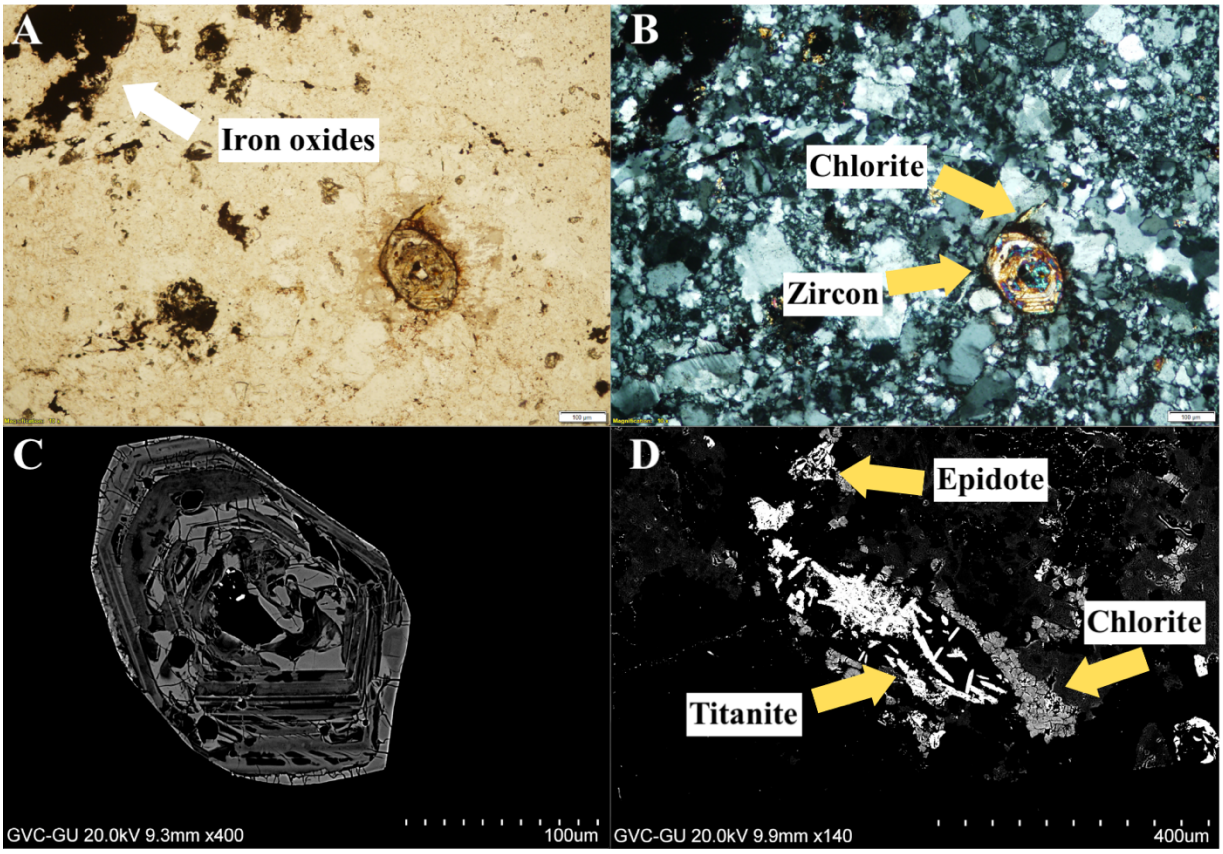


*Figure 15. Pictures of thin section 19FJ006. A) A large zoned zircon surrounded by small-grained quartz and smaller zircons. Photo taken in plane light. B) Same as in A, but photo taken in cross-polar light. Fractures around the zircon is filled with chlorite. C) Same as in A and B, photo taken in SEM. The zones are of different densities. The small white spots in the middle might be thorianite. D) A cluster of titanite surrounded by chlorite, K-feldspar and quartz and an epidote. Photo taken in SEM.*

Some fractures are filled with elongated light-yellow minerals (in plane light) and light colors in cross polar light (see figure 15A, B and C). When analyzed in SEM it indicated prehnite or clinochlore (Si-, Al- and Ca-rich).

Primary accessory minerals such as small grains of zircon or monazite was seen surrounded by an unidentified smaller grained matrix. These were hard to distinguish from each other in some areas, however a few clear grains were seen. When looked at in SEM microscope this was found out to be a matrix of iron oxides with zircons, and no monazites. The zircons had HFSE elements such as Hf, U and Th in it. However there was only very low concentrations of U.

No titanite was identified during regular microscopy, but with the SEM microscopy well-developed large titanite crystals was found. However these were fewer than in the thin section 19FJ006. Same with chlorite, this thin section consisted of less chlorite than the thin section 19FJ006.

### 3.4.2 19FJ006

The thin section has a large amount of chlorite, close to fractures. Opaques such as iron oxides can be seen together with minerals with higher relief. When looking at the thin section an influence of different events can be seen to have altered the sample, such as evidence with hydrothermal minerals but also fractures with filling.

In the sample, large quartz grains of mostly irregular shape (some hexagonal but not many) with undulatory extinction could be seen. Larger fractures in the thin section was filled with quartz crystals together with an outline border of a low relief brown mineral, identified in SEM as iron oxides. A few grains of K-feldspar with tartan twinning could be seen.

Chlorite with no sharp edges, surrounded by quartz, was green in plane light. In cross polar light the mineral was brownish in color with purple/pink areas enclosed. This might be the old biotite that the chlorite has altered from. When looked at in SEM this was confirmed to be chlorite and that a high quantity of the thin section consisted of chlorite, mainly around grain boundaries and fractures. More chlorite was found in thin section 19FJ006 than in 19FJ001.

Primary accessory minerals such as fairly large zircons (see figure 16) with high relief were found. These were colorless in plane light and showed a pink, green, blue shifting color with oscillatory zoning in cross polar light. More zircons could be seen in this thin section compared to thin section 19FJ001.

The zircons are surrounded by quartz, plagioclase and K-feldspar. In SEM these zircons showed different zones, containing the HFSE elements U, Hf and Th. In some grains most of the Th resided in the middle of the zircon, in what probably is thorianite. Tiny crystals of plagioclase and K-feldspar was found in the zircons, these might be left from a previous mineral. Fractures were seen emerging from the edges of the zircons filled with chlorite.

Opaques were distributed widespread in the thin section and many of the grains were found close to/together with chlorite. Next to epidote, chlorite, zircons and iron oxides small well shaped titanite and titanium oxide grains were identified. These grains lay in clusters surrounded by the previously mentioned minerals. When studied in SEM some titanite grains contained detectable but low concentrations of U, Ir and Nb.

# 4. Discussion

## 4.1 Radioactive elements

The spatial distribution of K, U and Th gave us high values of Th and K surrounding the Sahlgrenska anomaly and in Änggårdsbergen. The U concentrations are not high around Medicinareberget and the Sahlgrenska anomaly, but some areas are higher in Änggårdsbergen. Thorium is clearly increasing from east to west and it is high around the Sahlgrenska anomaly. This coincides well with previous studies where Th has been seen getting higher from east to west. The histograms (see figures 7C, 8C and 9C) indicates a normal distribution of values in the RA-granite in Änggårdsbergen for K, U and Th. The normal distribution shown in figure 7C, 8C and 9C is different from previously assumed RA-granite both according to SGU in table 1 but also according to Lundqvist et al (2011). Lundqvist et al (2011) presents the values of U (10-15 ppm) and Th (40-50 ppm) which is not correct according to our study. The normal distribution indicates that we now have enough measured values that represents RA-granite well.

As mentioned in section 3.1.6 compared to other granites (see figure 12) the RA-granite is more widely spread in both K- and Th-concentrations. When compared to the Stigfjord granite, it could be seen that the Stigfjord granite matches the RA-granite well in the amount of K, but has lower amounts of Th. All of this indicates that a similarity between the Bohus granite from Bohus-Malmön and RA-granite from Änggårdsbergen exists, and that the Stigfjord granite has similarities as well.

For the Th concentrations a clear enrichment in the Sahlgrenska anomaly/Medicinareberget could be seen. This indicates a local anomaly with enrichment of Th. Due to a lot of buildings in the Sahlgrenska University Hospital area and at Medicinareberget measurements were limited, so a more detailed anomaly border could not be seen. The anomaly might be more widespread, but this could not be measured. Sahlgrenska anomaly values of higher Th- and K-concentrations could indicate a local enrichment of Th and K in this area, with a leaching of U. According to Nash (1979) Th is generally immobile, which can coincide with the fact that Th-concentrations are high in some areas and U might have been mobilized. This might indicate that both concentrations have been high from the beginning, but U has moved. According to Musset and Khan (2000) hydrothermal events affect the mineral compositions during the crystallization and this could be when U and Th mobilizes.

U/Th ratios measured from the gamma spectrometry survey gave a clear evidence of possible hydrothermal events in various places in the combined field area (see figure 11). As mentioned before according to Musset and Khan (2000) a normal U/Th ratio in granite is 0.25. Many of the measurement sites of the gamma spectrometry gave a ratio below 0.25 and this might depend upon hydrothermal events affecting the mobilization of U. Hence this could also indicate oxidizing conditions, which has affected the U to mobilize (Musset & Khan, 2000). According to Musset and Khan (2000) U and Th are equally distributed in magmas, this is because of the reducing conditions in a melt. Therefore the "normal" ratio of U/Th in granites is about 0.25. If U or Th would have been unaffected in reducing conditions, we should therefore have had a ratio of 0.25, which we have in some areas. However Mernagh & Miezitis (2008) discusses that metamorphism might mobilize Th.

U/Th ratio in the rock samples (taken close to the Sahlgrenska anomaly) gave one ratio higher than 0.25 (19FJ001) and one

below (19FJ006). This might indicate that one of the samples could have been affected by hydrothermal events and the other not. However, combined with the result of gamma spectrometry ratios the lower ratios are well spread across the field area, but also spread when combined with previous studies. According to the U/Th ratio with values from gamma spectrometry for 19FJ001, the ratio was lower than 0.25. This might indicate that the ratios vary locally, and the rock samples are not taken at the exact same place as the gamma spectrometry measurements.

## 4.2 Susceptibility

The susceptibility values are the highest in the middle of Änggårdsbergen, but there is no correlation with the radioactive elements (see figure 13). According to Hultin and Håkansson (2018) but also Cooper Svensson and Lundin Frisk (2018) no correlation between the radioactive elements and susceptibility could be found. This matches well with the result of 2019.

## 4.3 Chemical analysis

According to Jiang et al. (2005) HFSE elements are usually resistant towards hydrothermal alteration and metamorphism, but this is probably not always the case. In some cases, the HFSE elements can be more or less mobile. Higher values of HFSE elements (Zr, Th) might indicate a presence of minerals such as zircon, monazite and allanite (Jiang et al., 2005). As was mentioned in section 3.4 both samples had zircon in them, this might be where the HFSE elements resides. When the thin sections were looked at in SEM microscope, Th, U and Hf (all HFSE) were identified residing in zircon. In the chemistry analysis concentrations of these were quite varied when combining all samples together. However this can depend upon the presence of zircon, monazite and allanite, and due to the amount of these minerals the concentrations of HFSE elements might vary.

Calculations made in section 3.3 showed that the rock samples are peraluminous. According to Bea (1996) accessory minerals of a peraluminous rock can be zircon and monazite. This matches well with finds from previous bachelor thesis (Hultin & Håkansson, 2018) but also the result of microscopy investigations of our thin sections, except from the lack of monazite. Bea (1996) also suggest that biotite indirectly control the geochemistry of REE, Th and U by including accessory minerals in it. However no biotite was found in our thin sections, but it may have become chloritized, and the elements may still be there but now included in chlorite instead. Uranium and thorium were found in zircons close to chlorite, but not in the chlorite itself. A study made on biotite in Japanese granite suggested that there are two ways for a chloritization to happen (Yuguchi et al.,2015). Both ways include a volume decrease when biotite gets chloritized. They differ in the way of large inflow of metallic ions from the hydrothermal fluid or large outflow of metallic ions into the hydrothermal fluid.

REE-bearing minerals such as monazite and allanite was found in previous year's studies in but not in ours. There might be allanite and monazite, but these could be very small. Cerium, which is usually part of allanite, was found scattered in the thin sections, maybe this is a rest of allanite. It may not be surprising that no allanite was found, since they are rare and easily altered (SGU, 2015). Due to no identification of allanite or monazite it has to be ruled out that U resides in these minerals. Low values of U were found in zircons and a few titanites. Based on the gamma spectrometry result and the chemical analysis more U was expected, but almost none was found in SEM.

However the concentrations might be too low to be detected in the SEM.

$SiO_2$ is the dominating major element of the rock, which was expected when a lot of feldspars and quartz was found in the thin sections, $SiO_2$ is also Th-bearing. Thorium was found in the SEM-microscope residing in zircon and the conclusion from this might be that some amount of Th in the rock is affected by $SiO_2$.
In figure 14 a negative Eu anomaly could be seen in all samples. Eu prefers to reside in plagioclase rather than in other minerals, so when plagioclase is crystallized and then separated, the rest of the magma becomes depleted in Eu (Weill and Drake, 1973). This is the case in our samples. A negative Eu anomaly may be expected and has been found in both previous bachelor theses (Hultin & Håkansson, 2018; Cooper Svensson & Lundin Frisk, 2018).

## 4.4 Microscopy and petrology

Chlorite found in thin section 19FJ006 might have been formed above 300 degrees during hydrothermal conditions. No biotite was found in the thin sections, only chlorite indicating that probably all biotite has been altered into chlorite. However, close to the chlorite red/brown iron oxides were found and according to Eggleton and Banfield (1985) the iron from the biotite might have been precipitated into the chlorite structure. But also, that the structure of biotite has been inherited by the chlorite. This could not be ruled out in our thin sections. Chlorite and iron oxides that lie around fractures are probably secondary crystallized, which may indicate a hydrothermal alteration of the previously magmatic rock.

Together with the chlorite, titanite was often found. As mentioned in section 3.4 the titanite grains were very small and surrounded by chlorite and epidote. The amount and the cluster of the titanite together with the smaller size might indicate a secondary crystallization in sample 19FJ006 and the size indicates a non-magmatic formation. During the chloritization of biotite Ti might be liberated and Ti oxides or Titanite would be created. This could explain how the secondary titanite and the Ti oxides were formed (SKB, 1993). In thin section 19FJ001 the titanite crystals were larger and more well developed, this might instead indicate a primary crystallization.

Many zircons were found in the regular microscope but the zircons in thin section 19FJ001 are not as big, developed grains and not as many as in the thin section 19FJ006. Although as mentioned in section 3.3 high values of Zr was found in the thin section 19FJ001, but this is also where fewer zircons resides. This could be due to the rock sample, not as many zircons in the rock sample as in the thin section.

Since both of our thin sections were collected close to the Sahlgrenska anomaly a comparison between those and the Sahlgrenska anomaly sample 16FF200 was made. According to Hultin and Håkansson (2018) the Sahlgrenska anomaly sample 16FF200 consisted mainly of different feldspars such as K-feldspar and plagioclase. Our samples seem to have more quartz than 16FF200 but still a fair amount of K-feldspar and plagioclase. 16FF200 had minerals of zircon, titanite, allanite, biotite, iron oxide and chlorite (Hultin and Håkansson, 2018). 16FF200 did not have as much fractures as our thin section samples. Our thin sections 19FJ001 and 19FJ006 showed no visible biotite but instead chlorite, and as mentioned before this might be due to chloritization of biotite. 19FJ001 and 19FJ006 are similar in many ways to 16FF200 - such as with where the radioactive elements reside, grain size, fractures and general mineralogy. All these three samples combined indicates a possible hydrothermal event with alteration.

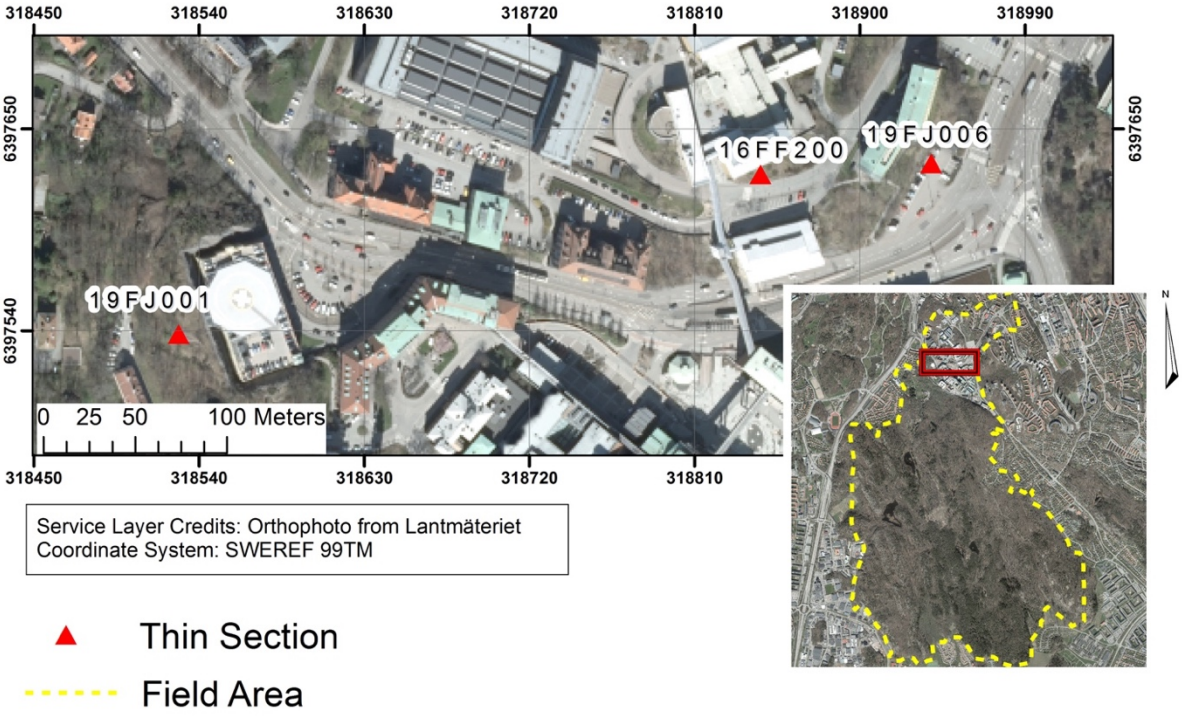


*Figure 16. Map of the thin sections closest to and including the Sahlgrenska anomaly (16FF200).*

Combining the information from regular microscopy and SEM a clear evidence of some kind of tectonic influence could be seen. Together with the proof of hydrothermal minerals (prehnite or clinochlore, chlorite and epidote), fractures and structures in the thin section we could say that the titanite and chlorite in thin section 19FJ006 probably has crystallized in some kind of secondary event. If so, something must have happened before this in order to let this happen. Fractures must have happened before these crystallizations when many of these minerals lay alongside or within fractures. Thin section 19FJ001 is geographically located further away from 16FF200 than thin section 19FJ006, see figure 17. Due to that, this local area might not have been as affected by a possible hydrothermal event as 19FJ006 and this might be why not as many chlorites and altered minerals were found in this one.

The most probable is that the fractures have developed during some kind of pressure change, such as a rifting event or an orogeny. If it is an orogeny that has affected the area, this could have been the Sveconorwegian, due to this being the only one of the two orogenesis happening in the area that could possibly have affected the RA-granite. Metamorphism might have happened at the same time as this or in the period after the Sveconorwegian orogeny and a hydrothermal event might have taken place after these events together with filling up fractures. According to SGU (2015) there are two ways for U and Th to be enriched in a rock. In magmatic rock forming processes U and Th are enriched in late crystallized magmas. Granites formed due to partial melting of older crust related to orogenies will generally have higher content of U and Th than the parent rock. We know that the RA-granite has been affected by the Sweconorweigan orogeny, so this matches well with the enrichment of U and Th.

## 4.5 Sources of error

When measuring with gamma ray spectrometry the geometry of the rock wall is important. Geometry errors might be seen within Änggårdsbergen due to some areas with not as optimal rock walls as others, but it is hard to distinguish from previous years data when we have not seen

the measurement sites. Though the study of 2019 had a focus on the scale from SGU (0-3) with good quality measuring sites rather than many with bad quality. At the Sahlgrenska University Hospital area the best sites that were found were chosen, but these sites were small. The sites in Änggårdsbergen/Gothenburg Botanical Garden were larger and therefore better.

Interpolation was made both for RA-granite and for areas with no RA-granite. Measurement sites within Änggårdsbergen where other rock types existed were removed as well as could be however, with a large amount of data some points might still be there affecting the interpolation values.

When the interpolation maps were created, some of the sample points seem as isolated anomalies. However if these have no additional sampling points between each other these might be the same anomaly.

## 4.6 Further research

The RA-granite in Änggårdsbergen has now been well mapped and the result of all combined studies might act as normal values for RA-granite. However, we encourage more mapping of the contact between the RA-granite and other bedrock plus further studies with focuses on the Sahlgrenska anomaly – where dating of the possibly secondary titanites containing U might be done. This could give a time frame of when a hydrothermal event might have taken place.

# 5. Conclusions

- The spatial distribution of K, U and Th is well mapped, and the result might work as a "normal RA-granite". The normal values are 3.5-5 % for K, 7-18 ppm for U and 30-70 ppm for Th.
- Based on the radiometric concentrations the Sahlgrenska anomaly is clearly isolated.
- When combining gamma spectrometry, microscopy and U/Th ratios it gives a clear picture of a hydrothermal event surrounding/at the Sahlgrenska anomaly.
- Implications of tectonic events exists as structures in the thin sections, combined together with knowledge of the regional geology, however it is hard to guess when the events took place, but it is possible to put in a chronological order.

# References


Ackevall, E. (2016). *U-Pb and Hf isotopes of zircon from a bimodal dyke at Lotsutkiken, Sweden: Implications for tectonic interpretations of the Idefjorden Terrane.* (Master thesis). Gothenburg: Department of Earth Sciences, University of Gothenburg. Available: https://studentportal.gu.se/digitalAssets/1571/1571755_b904.pdf

Aspfors, H. (red.) (1999). *Berggrundsbeskrivning av Slottsskogen och Änggårdsbergen*. (ISSN: 1400-383X, C18). Gothenburg: University of Gothenburg.

Austin Hegardt, E., Cornell, D.H., Hellström, F.A., & Lundqvist, I. (2007). Emplacement ages of the mid-Proterozoic Kungsbacka Bimodal Suite, SW Sweden. *GFF*, *129*(3), 227-234. DOI: 10.1080/11035890701293227

Bea, F. (1996). Residence of REE, Y, Th and U in Granites and Crustal Protoliths; Implications for the Chemistry of Crustal Melts. Journal of Petrology, 37(3), 521-552. DOI: 10.1093/petrology/37.3.521

Berger B.R. (1998). Hydrothermal alteration. In: *Geochemistry. Encyclopedia of Earth Science*. Dordrecht: Springer,. DOI: https://doi.org/10.1007/1-4020-4496-8_162

Best, M. G. (2003). *Igneous and metamorphic petrology* (2. ed.). Malden: Blackwell Publishers.

Bruhn, R.L., Parry, W.T., Yonkee, W.A., & Thompson, T. (1994). Fracturing and hydrothermal alteration in normal fault zones. *PAGEOPH, 142*(3-4), 609-644. https://doi.org/10.1007/BF00876057

Cooper Svensson, J. & Lundin Frisk, E. (2018). *Geofysisk och geokemisk kartering av kalium-, uran- och toriumkoncentrationer i Kärrragranit inom Änggårdsbergen, Göteborg.* (Bachelor thesis). Gothenburg: Department of Earth Sciences, University of Gothenburg.

Eggleton, R.A., & Banfield, J.F. (1985). The alteration of granitic biotite to chlorite. *American Mineralogist, 70*(9), 902-910.

Hultin, N. & Håkansson, A. (2018). *Spatial variation of K-, U- and Th-concentrations in RA-granite at Änggårdsbergen, southern Gothenburg.* (Bachelor thesis). Gothenburg: Department of Earth Sciences, University of Gothenburg. Available: https://studentportal.gu.se/digitalAssets/1686/1686486_b989.pdf

Jiang, S.Y., Wang, R.C., Xu, X.S., & Zhao, K.D. (2005). Mobility of high field strength elements (HFSE) in magmatic-, metamorphic-, and submarine-hydrothermal systems. *Physics and Chemistry of the Earth, 30*(17-18 SPEC. ISS), 1020-1029.

Johansson, J. (2018). *U och Th fördelning i Bohusgraniten på Bohus-Malmön.* (Bachelor thesis). Gothenburg: Department of Earth Sciences, University of Gothenburg. Available: https://studentportal.gu.se/digitalAssets/1512/1512705_b842.pdf

Lundqvist, J., Lundqvist, T., & Lindström, M. (2011). *Sveriges geologi från urtid till nutid*. Lund: Studentlitteratur.

Länsstyrelsen. (N.d.). *Änggårdsbergen*. Retrieved 2019-04-30 from https://www.lansstyrelsen.se/vastra-gotaland/besok-och-upptack/naturreservat/anggardsbergen.html

Mernagh, T.P. & Miezitis, Y. (2008). *A review of the geochemical processes controlling the distribution of thorium in the Earth's crust and Australia's thorium resources.* Canberra: Geoscience Australia.

Mussett, A.E. & Khan, M.A. (2000). *Looking into the earth: an introduction to geological geophysics*. Cambridge: Cambridge University Press.

Nash, J.T. (1979). *Uranium and thorium in granitic rocks of northeastern Washington and northern Idaho, with comments on uranium resource potential.* (Open-File Report, 79-233). U.S. Geological Survey. DOI: https://doi.org/10.3133/ofr79233

SGU. (2015). *Strålning från bergmaterial*. Stockholm: Sveriges Geologiska Undersökning.

SKB. (1993). *Mineralogy, geochemistry and petrophysics of red coloured granite adjacent to fractures*. Gothenburg: Chalmers University of Technology and University of Göteborg.

Taylor, S.R. & McLennan, S.M. (1985). *The continental crust: its composition and evolution: an examination of the geochemical record preserved in sedimentary rocks*. Oxford: Blackwell Scientific.

Weill, D.F. & Drake, M.J. (1973). Europium Anomaly in Plagioclase Feldspar: Experimental Results and Semiquantitative Model. *Science, 180*(4090), 1059-1060. DOI: 10.1126/science.180.4090.1059

Yuguchi, T., Sasao, E., Ishibashi, M. & Nishiyama T. (2015). Hydrothermal chloritization processes from biotite in the Toki granite, Central Japan: Temporal variations of the compositions of hydrothermal fluids associated with chloritization. *American Mineralogist, 100*(5-6), 1134-1152. https://doi.org/10.2138/am-2015-5126

# Appendix

**A. Concentrations of elements for all rock samples taken in Änggårdsbergen in RA-granite.**

| Elements | Unit | 19FJ001 | 19FJ006 | 19FJ055 | 19FJ056 | 16FF200 | 17ANH009 | 17ANH030 | 17FF02 | 17FF04 | 18AJE1 | 18AJE2 | 18AJE3 | 18AJE4 | 18AJE5 | 18AJE6 |
|---|---|---|---|---|---|---|---|---|---|---|---|---|---|---|---|---|
| $SiO_2$ | % | 81 | 65.4 | 74.8 | 73.8 | 61.7 | 77 | 77.3 | 74.4 | 76.1 | 75.8 | 73 | 74.5 | 73.3 | 79.5 | 77.7 |
| $Al_2O_3$ | % | 9 | 17.5 | 12.95 | 12.5 | 17.15 | 11.65 | 11.9 | 12.3 | 10.55 | 12.7 | 12.35 | 11.7 | 11.9 | 10.65 | 11.05 |
| $Fe_2O_3$ | % | 4.22 | 2.45 | 2.65 | 4.59 | 5.21 | 1.99 | 1.52 | 4.04 | 4.38 | 2.17 | 3.14 | 2.89 | 3.77 | 1.63 | 1.75 |
| CaO | % | 0.31 | 0.78 | 0.9 | 0.2 | 0.28 | 0.21 | 0.43 | 0.5 | 0.13 | 0.4 | 0.38 | 0.14 | 0.12 | 0.06 | 0.14 |
| MgO | % | 0.22 | 1.29 | 0.2 | 0.04 | 0.6 | 0.24 | 0.22 | 0.02 | 0.03 | 0.28 | 0.31 | 0.02 | 0.03 | 0.24 | 0.18 |
| $Na_2O$ | % | 2.27 | 5.33 | 3.55 | 3.94 | 1.58 | 3.78 | 2.63 | 3.69 | 4.04 | 3.95 | 3.72 | 3.68 | 3.99 | 2.63 | 2.57 |
| $K_2O$ | % | 3.82 | 5.91 | 5.02 | 4.82 | 11.95 | 4.38 | 5.48 | 5.03 | 4.95 | 4.42 | 5.01 | 5 | 5.39 | 4.87 | 5.12 |
| $Cr_2O_3$ | % | 0.004 | 0.004 | 0.003 | 0.003 | <0.01 | <0.01 | <0.01 | <0.01 | <0.01 | 0.024 | 0.01 | 0.01 | 0.01 | 0.013 | 0.01 |
| $TiO_2$ | % | 0.21 | 0.38 | 0.22 | 0.37 | 0.49 | 0.23 | 0.22 | 0.36 | 0.3 | 0.22 | 0.33 | 0.27 | 0.31 | 0.22 | 0.2 |
| MnO | % | 0.03 | 0.02 | 0.04 | 0.01 | 0.03 | 0.02 | 0.02 | 0.05 | 0.07 | 0.03 | 0.03 | 0.03 | 0.06 | 0.02 | 0.02 |
| $P_2O_5$ | % | 0.01 | 0.05 | 0.02 | 0.01 | 0.03 | 0.02 | 0.03 | 0.03 | 0.01 | 0.04 | 0.02 | 0.02 | 0.01 | 0.02 | 0.03 |
| SrO | % | <0.01 | 0.01 | <0.01 | <0.01 | <0.01 | <0.01 | <0.01 | <0.01 | <0.01 | <0.01 | <0.01 | <0.01 | <0.01 | <0.01 | <0.01 |
| BaO | % | <0.01 | 0.05 | 0.02 | <0.01 | 0.03 | 0.02 | 0.01 | 0.01 | <0.01 | 0.02 | 0.01 | <0.01 | <0.01 | 0.01 | 0.01 |
| LOI | % | 0.44 | 1.09 | 0.56 | 0.41 | 1.23 | 0.48 | 0.65 | 0.16 | 0.09 | 0.77 | 0.63 | 0.39 | 0.21 | 0.86 | 0.63 |
| Total | % | 101.53 | 100.27 | 100.93 | 100.69 | 100.28 | 100.02 | 100.41 | 100.57 | 100.65 | 100.82 | 98.94 | 98.65 | 99.1 | 100.72 | 99.41 |
| C | % | 0.02 | 0.01 | 0.03 | 0.02 | 0.07 | 0.03 | 0.06 | 0.01 | 0.01 | 0.03 | 0.05 | 0.05 | 0.05 | 0.02 | 0.1 |
| S | % | 0.01 | 0.01 | 0.01 | <0.01 | 0.01 | 0.01 | <0.01 | <0.01 | <0.01 | <0.01 | <0.01 | <0.01 | <0.01 | <0.01 | <0.01 |
| Ba | ppm | 41.6 | 479 | 164.5 | 43 | 256 | 133 | 87.5 | 49.3 | 23.1 | 168.5 | 67.3 | 26.4 | 31 | 91.7 | 94.3 |

| | | | | | | | | | | | | | | | | |
|---|---|---|---|---|---|---|---|---|---|---|---|---|---|---|---|---|
| **Ce** | **ppm** | **219** | **136** | **265** | **334** | **889** | **180** | **23.9** | **411** | **240** | **162.5** | **344** | **205** | **160.5** | **36.1** | **43.6** |
| **Cr** | **ppm** | **20** | **20** | **20** | **10** | **<10** | **<10** | **<10** | **10** | **<10** | **160** | **60** | **60** | **50** | **100** | **90** |
| **Cs** | **ppm** | **1.53** | **2.64** | **4.94** | **2.41** | **4.13** | **0.87** | **9.04** | **1.36** | **4** | **1.3** | **1.3** | **2.18** | **7.98** | **4.23** | **4.41** |
| **Dy** | **ppm** | **22.5** | **7.19** | **20.6** | **23** | **56.2** | **9.35** | **6.57** | **32.5** | **20** | **12.75** | **20.9** | **18.5** | **17.6** | **6.03** | **4.04** |
| **Er** | **ppm** | **17.05** | **4.62** | **13.35** | **13.95** | **30.4** | **6.73** | **5.46** | **17.55** | **13.5** | **7.74** | **13.3** | **11.75** | **12.7** | **5.3** | **3.44** |
| **Eu** | **ppm** | **0.71** | **0.72** | **1.01** | **1.25** | **3.19** | **0.44** | **0.14** | **1.73** | **0.71** | **0.71** | **1.01** | **0.68** | **0.53** | **0.12** | **0.06** |
| **Ga** | **ppm** | **26.8** | **17.2** | **34.4** | **42** | **22.5** | **26** | **16.8** | **39.3** | **40.8** | **29.4** | **37.2** | **37.9** | **42.1** | **15.1** | **15.3** |
| **Gd** | **ppm** | **16.7** | **7.38** | **17.45** | **23.1** | **58.9** | **7.62** | **3.06** | **30.2** | **14.95** | **12.05** | **18.45** | **13** | **9.78** | **3.44** | **1.54** |
| **Ge** | **ppm** | **<5** | **<5** | **<5** | **<5** | **<5** | **<5** | **<5** | **<5** | **<5** | **<5** | **<5** | **<5** | **<5** | **<5** | **<5** |
| **Hf** | **ppm** | **40.8** | **6.8** | **15.3** | **32.9** | **42.8** | **24** | **7** | **34.8** | **57.3** | **11** | **25.6** | **37.4** | **34.8** | **6.7** | **6** |
| **Ho** | **ppm** | **5.42** | **1.52** | **4.15** | **4.73** | **10.35** | **2.09** | **1.6** | **6.04** | **4.12** | **2.5** | **4.44** | **4** | **3.99** | **1.53** | **1** |
| **La** | **ppm** | **88.2** | **73.1** | **122.5** | **149** | **405** | **74.7** | **9.3** | **169.5** | **99.5** | **89.6** | **166.5** | **98.2** | **41.5** | **8.9** | **7.6** |
| **Lu** | **ppm** | **2.57** | **0.72** | **2.21** | **1.93** | **3.86** | **1.31** | **1.14** | **2.45** | **2.45** | **1.14** | **2.05** | **1.86** | **2.48** | **0.91** | **0.73** |
| **Nb** | **ppm** | **96.4** | **17.4** | **88.3** | **64** | **113.5** | **59.5** | **26.9** | **74.6** | **157.5** | **56.3** | **94.1** | **129** | **123** | **19.6** | **17.9** |
| **Nd** | **ppm** | **81** | **47.6** | **108.5** | **151.5** | **326** | **60.6** | **8.5** | **162** | **80.4** | **77.4** | **128.5** | **82.8** | **41.2** | **8.7** | **6** |
| **Pr** | **ppm** | **22.7** | **15.46** | **29.4** | **38.9** | **91.3** | **16.8** | **2.45** | **42.6** | **22.1** | **21.1** | **36.1** | **23.7** | **10.85** | **2.55** | **1.68** |
| **Rb** | **ppm** | **307** | **262** | **454** | **254** | **679** | **204** | **446** | **305** | **548** | **299** | **395** | **448** | **518** | **416** | **363** |
| **Sm** | **ppm** | **17.6** | **8.27** | **21.1** | **28.4** | **63.7** | **11.1** | **2.54** | **34.1** | **15.95** | **14.5** | **24.6** | **18.3** | **10.45** | **2.45** | **1.44** |
| **Sn** | **ppm** | **21** | **5** | **14** | **14** | **14** | **5** | **7** | **17** | **42** | **10** | **25** | **24** | **25** | **7** | **5** |
| **Sr** | **ppm** | **15.5** | **88.1** | **35.5** | **16.5** | **37** | **36.6** | **23.4** | **24.7** | **2.8** | **27.8** | **19** | **4.5** | **2.4** | **19.2** | **24.8** |
| **Ta** | **ppm** | **6.4** | **1.7** | **5.6** | **2.7** | **10.1** | **3.8** | **2.4** | **5.2** | **11.8** | **4.1** | **6.2** | **6.9** | **8.3** | **2.2** | **2** |
| **Tb** | **ppm** | **3.32** | **1.18** | **3.31** | **3.96** | **9.36** | **1.42** | **0.84** | **5.26** | **2.87** | **2.01** | **3.41** | **2.64** | **2.28** | **0.78** | **0.49** |

| | | | | | | | | | | | | | | | | |
|---|---|---|---|---|---|---|---|---|---|---|---|---|---|---|---|---|
| **Th** | **ppm** | **49.9** | **55.4** | **47.9** | **32.9** | **201** | **56.6** | **60.6** | **42.4** | **79.6** | **41** | **55.4** | **66.9** | **63.1** | **77.3** | **63.1** |
| **Tm** | **ppm** | **2.88** | **0.73** | **2.01** | **1.9** | **4.46** | **1.19** | **1.01** | **2.66** | **2.28** | **1.26** | **2.08** | **1.88** | **2.16** | **0.89** | **0.69** |
| **U** | **ppm** | **14.05** | **10.9** | **12.4** | **7.58** | **19.35** | **9.17** | **19.7** | **10.15** | **14.85** | **12.4** | **11.3** | **13.7** | **10.45** | **7.61** | **7.3** |
| **V** | **ppm** | **18** | **39** | **12** | **<5** | **34** | **9** | **11** | **<5** | **<5** | **17** | **10** | **5** | **<5** | **8** | **10** |
| **W** | **ppm** | **2** | **1** | **2** | **3** | **1** | **1** | **4** | **<1** | **2** | **1** | **2** | **1** | **1** | **<1** | **1** |
| **Y** | **ppm** | **147.5** | **44** | **116** | **120.5** | **306** | **60.3** | **45.3** | **173.5** | **121** | **65** | **125** | **104.5** | **86.2** | **46.1** | **30.2** |
| **Yb** | **ppm** | **18.55** | **5.11** | **14.05** | **12.05** | **27.2** | **8.45** | **7.33** | **16.75** | **15.8** | **8.61** | **14** | **12.75** | **15.6** | **7** | **4.72** |
| **Zr** | **ppm** | **1600** | **216** | **429** | **1315** | **1625** | **862** | **172** | **1375** | **1865** | **292** | **881** | **1200** | **1210** | **171** | **151** |
| **As** | **ppm** | **1.3** | **0.1** | **0.5** | **0.6** | **0.1** | **3.7** | **0.4** | **0.2** | **<0.1** | **4.3** | **3.4** | **4.9** | **5.7** | **2.4** | **6.2** |
| **Bi** | **ppm** | **0.16** | **0.22** | **0.22** | **0.32** | **0.12** | **0.61** | **0.08** | **0.12** | **1.26** | **0.17** | **0.09** | **0.42** | **1.04** | **0.13** | **0.1** |
| **Hg** | **ppm** | **0.017** | **0.011** | **0.006** | **0.007** | **<0.005** | **<0.005** | **<0.005** | **<0.005** | **<0.005** | **0.005** | **0.012** | **0.012** | **<0.005** | **<0.005** | **<0.005** |
| **In** | **ppm** | **0.23** | **0.026** | **0.107** | **0.172** | **0.043** | **0.054** | **0.008** | **0.195** | **0.014** | **0.043** | **0.138** | **0.145** | **0.022** | **0.013** | **0.009** |
| **Re** | **ppm** | **0.004** | **0.002** | **0.006** | **0.003** | **0.001** | **0.001** | **<0.001** | **0.001** | **<0.001** | **0.001** | **0.001** | **0.001** | **0.001** | **<0.001** | **0.001** |
| **Sb** | **ppm** | **0.14** | **0.09** | **0.07** | **0.09** | **<0.05** | **0.1** | **0.07** | **<0.05** | **<0.05** | **<0.05** | **<0.05** | **<0.05** | **<0.05** | **<0.05** | **<0.05** |
| **Se** | **ppm** | **0.2** | **0.3** | **0.4** | **0.7** | **4.9** | **1** | **1** | **4** | **2.5** | **<0.2** | **<0.2** | **<0.2** | **0.2** | **<0.2** | **<0.2** |
| **Te** | **ppm** | **0.02** | **<0.01** | **<0.01** | **0.01** | **0.01** | **0.62** | **0.01** | **<0.01** | **0.01** | **0.01** | **0.01** | **<0.01** | **<0.01** | **<0.01** | **<0.01** |
| **Tl** | **ppm** | **0.04** | **0.03** | **0.76** | **0.04** | **0.07** | **0.06** | **0.19** | **0.06** | **0.14** | **0.06** | **0.08** | **0.23** | **0.09** | **0.04** | **0.04** |
| **Ag** | **ppm** | **<0.5** | **<0.5** | **<0.5** | **<0.5** | **<0.5** | **0.5** | **<0.5** | **<0.5** | **<0.5** | **<0.5** | **<0.5** | **1.2** | **1.1** | **<0.5** | **<0.5** |
| **Cd** | **ppm** | **<0.5** | **<0.5** | **<0.5** | **<0.5** | **<0.5** | **<0.5** | **<0.5** | **<0.5** | **<0.5** | **<0.5** | **<0.5** | **<0.5** | **<0.5** | **<0.5** | **<0.5** |
| **Co** | **ppm** | **2** | **5** | **3** | **2** | **4** | **1** | **2** | **<1** | **1** | **1** | **<1** | **1** | **<1** | **1** | **<1** |
| **Cu** | **ppm** | **12** | **85** | **8** | **21** | **3** | **10** | **2** | **12** | **4** | **8** | **2** | **7** | **1** | **3** | **<1** |
| **Li** | **ppm** | **<10** | **10** | **20** | **<10** | **<10** | **<10** | **10** | **<10** | **120** | **10** | **10** | **<10** | **60** | **20** | **10** |

| | | | | | | | | | | | | | | | | |
|---|---|---|---|---|---|---|---|---|---|---|---|---|---|---|---|---|
| **Mo** | **ppm** | **2** | **<1** | **6** | **3** | **<1** | **1** | **<1** | **2** | **<1** | **4** | **<1** | **2** | **1** | **<1** | **1** |
| **Ni** | **ppm** | **2** | **6** | **6** | **4** | **4** | **1** | **<1** | **1** | **1** | **2** | **4** | **2** | **2** | **<1** | **4** |
| **Pb** | **ppm** | **20** | **22** | **68** | **9** | **41** | **15** | **29** | **29** | **58** | **44** | **28** | **38** | **41** | **57** | **26** |
| **Sc** | **ppm** | **<1** | **5** | **1** | **<1** | **5** | **1** | **2** | **1** | **<1** | **1** | **1** | **1** | **1** | **2** | **2** |
| **Zn** | **ppm** | **95** | **32** | **117** | **20** | **57** | **21** | **21** | **119** | **270** | **55** | **153** | **91** | **237** | **28** | **18** |

B. Table for the measured border of the RA-granite.

| Point | Lon. | Lat. |
|---|---|---|
| 1 | 11.963242 | 57.684522 |
| 2 | 11.962361 | 57.684824 |
| 3 | 11.961868 | 57.684902 |
| 4 | 11.960135 | 57.684753 |
| 5 | 11.957726 | 57.685459 |
| 6 | 11.95755 | 57.684970 |
| 7 | 11.95627 | 57.686100 |

C. Gamma spectrometry and susceptibility measurements from all the three bachelor theses studying Änggårdsbergen and additional measurements by Professor Erik Sturkell. Red marking means it has not been used for interpolation.

| Location | | | Gamma spectrometry | | | | Susceptibility | | | | SGU |
|---|---|---|---|---|---|---|---|---|---|---|---|
| ID | Lon. | Lat. | K (%) | U (ppm) | Th (ppm) | U/ Th | Value | Mean/ Median | Min | Max | Scale |
| 19FJ001 | 11.9561 | 57.6834 | 4.4 | 11.7 | 57.0 | 0.21 | 32.5 | Median | 2 | 60 | 2 |
| 19FJ003 | 11.9534 | 57.678 | 4.3 | 9.2 | 33.2 | 0.28 | 750 | Median | 600 | 1250 | 3 |
| 19FJ004 | 11.9572 | 57.6863 | 2.5 | 2.2 | 6.4 | 0.34 | - | Median | - | - | 2 |
| 19FJ005 | 11.9601 | 57.6843 | 5.2 | 11.8 | 71.9 | 0.16 | - | Median | - | - | 2 |
| 19FJ006 | 11.9629 | 57.6844 | 5.0 | 10.3 | 56.0 | 0.18 | - | Median | - | - | 3 |
| 19FJ007 | 11.96813 | 57.68975 | 2.1 | 1.4 | 9.4 | 0.15 | 220 | Median | 10 | 400 | 3 |
| 19FJ008 | 11.967451 | 57.689865 | 2.6 | 1.8 | 7.8 | 0.23 | 150 | Median | 52.5 | 600 | 3 |
| 19FJ009 | 11.958240 | 57.686900 | 3.4 | 3.7 | 15.9 | 0.23 | 450 | Median | 125 | 550 | 2 |
| 19FJ010 | 11.958787 | 57.685408 | 4.8 | 1.7 | 1.1 | 1.53 | - | Median | - | - | 3 |
| 19FJ011 | 11.960279 | 57.683991 | 2.2 | 7.8 | 28.1 | 0.28 | 50 | Median | 10 | 65 | 3 |
| 19FJ012 | 11.961216 | 57.684288 | 7.1 | 12.9 | 61.1 | 0.21 | 40 | Median | 12.5 | 80 | 3 |
| 19FJ013 | 11.957852 | 57.681952 | 4.9 | 4.8 | 28.2 | 0.17 | 20 | Median | 10 | 70 | 1 |
| 19FJ014 | 11.952638 | 57.682552 | 4.3 | 8.6 | 31.3 | 0.28 | 500 | Median | 40 | 750 | 3 |
| 19FJ015 | 11.952664 | 57.679133 | 4.0 | 15.0 | 27.2 | 0.55 | 500 | Median | 500 | 800 | 3 |
| 19FJ016 | 11.952791 | 57.678606 | 4.4 | 10.1 | 29.5 | 0.34 | 625 | Median | 500 | 1000 | 3 |
| 19FJ017 | 11.943108 | 57.675529 | 4.4 | 16.8 | 64.4 | 0.26 | 325 | Median | 300 | 475 | 2 |
| 19FJ018 | 11.943163 | 57.674924 | 4.5 | 15.4 | 64.0 | 0.24 | 350 | Median | 55 | 550 | 3 |
| 19FJ019 | 11.943961 | 57.674608 | 4.3 | 16.0 | 59.8 | 0.27 | 350 | Median | 125 | 750 | 3 |
| 19FJ020 | 11.946669 | 57.672953 | 4.4 | 18.1 | 61.7 | 0.29 | 375 | Median | 32 | 450 | 3 |
| 19FJ021 | 11.946072 | 57.670990 | 4.3 | 12.8 | 59.5 | 0.22 | 600 | Median | 375 | 725 | 3 |
| 19FJ022 | 11.947366 | 57.670115 | 4.5 | 14.9 | 63.0 | 0.24 | 400 | Median | 300 | 700 | 3 |
| 19FJ023 | 11.947665 | 57.667365 | 5.8 | 13.9 | 78.4 | 0.18 | 10 | Median | 0 | 17.5 | 3 |
| 19FJ024 | 11.951276 | 57.671933 | 4.1 | 11.8 | 47.3 | 0.25 | 2500 | Median | 10 | 3000 | 3 |
| 19FJ025 | 11.950691 | 57.674396 | 4.6 | 17.1 | 67.0 | 0.26 | 1500 | Median | 1000 | 2000 | 1 |
| 19FJ026 | 11.949795 | 57.676292 | 4.5 | 9.2 | 44.3 | 0.21 | 4000 | Median | 2000 | 4250 | 1 |
| 19FJ027 | 11.948522 | 57.676594 | 4.4 | 17.5 | 67.7 | 0.26 | 1000 | Median | 100 | 2000 | 3 |
| 19FJ028 | 11.961203 | 57.688250 | 5.0 | 3.1 | 6.1 | 0.50 | 0 | Median | 0 | 25 | 3 |
| 19FJ029 | 11.960746 | 57.687865 | 3.1 | 3.3 | 9.2 | 0.36 | 350 | Median | 50 | 400 | 3 |
| 19FJ030 | 11.958529 | 57.688509 | 3.9 | 6.9 | 10.7 | 0.65 | 0 | Median | 0 | 300 | 3 |
| 19FJ031 | 11.956623 | 57.688434 | 1.4 | 4.4 | 8.7 | 0.51 | - | Median | - | - | 3 |
| 19FJ032 | 11.960087 | 57.684864 | 2.6 | 2.2 | 8.1 | 0.27 | 400 | Median | 400 | 450 | 3 |
| 19FJ033 | 11.957386 | 57.683019 | 3.4 | 6.8 | 23.8 | 0.29 | 15 | Median | 0 | 20 | 3 |
| 19FJ034 | 11.953889 | 57.680147 | 4.6 | 9.5 | 37.3 | 0.25 | 550 | Median | 200 | 1000 | 1 |
| 19FJ035 | 11.952717 | 57.676596 | 4.7 | 11.2 | 42.7 | 0.26 | 800 | Median | 200 | 950 | 3 |
| 19FJ036 | 11.952366 | 57.675338 | 4.4 | 8.7 | 42.5 | 0.21 | 2000 | Median | 1750 | 3000 | 3 |
| 19FJ037 | 11.951323 | 57.671597 | 4.5 | 10.8 | 52.3 | 0.21 | 2500 | Median | 950 | 3000 | 3 |
| 19FJ038 | 11.948164 | 57.666718 | 4.4 | 11.2 | 59.4 | 0.19 | 40 | Median | 30 | 70 | 3 |
| 19FJ039 | 11.946068 | 57.667978 | 3.7 | 2.4 | 13.4 | 0.18 | 1000 | Median | 50 | 1750 | 3 |
| 19FJ040 | 11.947920 | 57.669319 | 4.2 | 15.8 | 63.9 | 0.25 | 400 | Median | 100 | 700 | 3 |
| 19FJ041 | 11.948432 | 57.670000 | 4.4 | 16.4 | 62.8 | 0.26 | 300 | Median | 100 | 500 | 3 |
| 19FJ042 | 11.949783 | 57.673051 | 4.2 | 29.4 | 41.8 | 0.70 | - | Median | - | - | 3 |
| 19FJ043 | 11.949284 | 57.673440 | 3.1 | 14.4 | 56.8 | 0.25 | - | Median | - | - | 3 |
| 19FJ044 | 11.94847 | 57.673898 | 4.0 | 15.8 | 54.3 | 0.29 | - | Median | - | - | 3 |
| 19FJ045 | 11.948072 | 57.675684 | 5.0 | 20.4 | 74.7 | 0.27 | - | Median | - | - | 3 |
| 19FJ046 | 11.945382 | 57.673928 | 4.6 | 16.0 | 67.7 | 0.24 | 5 | Median | 0 | 65 | 3 |

| | | | | | | | | | | | |
|---|---|---|---|---|---|---|---|---|---|---|---|
| 19FJ047 | 11.944406 | 57.672918 | 4.4 | 8.2 | 59.0 | 0.14 | 0 | Median | 0 | 100 | 3 |
| 19FJ048 | 11.950866 | 57.677843 | 4.3 | 8.3 | 31.1 | 0.27 | 1000 | Median | 650 | 1000 | 3 |
| 19FJ049 | 11.952742 | 57.679862 | 4.4 | 9.4 | 28.6 | 0.33 | 1000 | Median | 100 | 1500 | 1 |
| 19FJ050 | 11.960703 | 57.680434 | 3.8 | 7.6 | 21.4 | 0.35 | 525 | Median | 0 | 1500 | 1 |
| 19FJ051 | 11.961986 | 57.680602 | 5.3 | 9.4 | 37.8 | 0.25 | 0 | Median | 0 | 15 | 3 |
| 19FJ052 | 11.965611 | 57.679889 | 6.6 | 14.6 | 71.6 | 0.20 | 0 | Median | 0 | 70 | 2 |
| 19FJ053 | 11.965445 | 57.681651 | 3.0 | 7.3 | 15.2 | 0.48 | 0 | Median | 0 | 30 | 3 |
| 19FJ054 | 11.964024 | 57.684692 | 3.1 | 4.7 | 14.4 | 0.33 | - | Median | - | - | 3 |
| 19FJ056 | 11.957613 | 57.684009 | 4.1 | 9.9 | 41.7 | 0.24 | 250 | Median | 150 | 1500 | 3 |
| 19FJ057 | 11.959855 | 57.681690 | 5.3 | 9.8 | 48.4 | 0.20 | - | Median | - | - | 3 |
| 19FJ058 | 11.960596 | 57.681447 | 5.1 | 10.4 | 50.7 | 0.21 | 0 | Median | 0 | 250 | 3 |
| 1 | 11.96469 | 57.67402 | 3.9 | 12.4 | 41.5 | 0.30 | - | Mean | - | - | - |
| 2 | 11.96575 | 57.67342 | 4.5 | 13.3 | 47.1 | 0.28 | - | Mean | - | - | - |
| 3 | 11.96679 | 57.67185 | 4.7 | 10.4 | 54.1 | 0.19 | - | Mean | - | - | - |
| 4 | 11.96869 | 57.67039 | 4.4 | 7.6 | 31.5 | 0.24 | 143.33 | Mean | 10 | 500 | - |
| 5 | 11.97184 | 57.66972 | 4.0 | 16.1 | 46.6 | 0.35 | 163.75 | Mean | 0 | 350 | - |
| 6 | 11.96985 | 57.66975 | 4.5 | 8.4 | 35.1 | 0.24 | 542.50 | Mean | 380 | 650 | - |
| 7 | 11.97358 | 57.66785 | 4.1 | 18.0 | 48.1 | 0.37 | 149.92 | Mean | 22 | 350 | - |
| 8 | 11.97787 | 57.66516 | 4.5 | 12.5 | 48.6 | 0.26 | 298.33 | Mean | 190 | 400 | - |
| 9 | 11.97979 | 57.66333 | 4.1 | 12.5 | 46.6 | 0.27 | 290.83 | Mean | 100 | 420 | - |
| 10 | 11.98106 | 57.66214 | 4.3 | 12.7 | 47.5 | 0.27 | 382.50 | Mean | 50 | 730 | - |
| 11 | 11.98506 | 57.6619 | 4.4 | 12.5 | 48.5 | 0.26 | 356.67 | Mean | 300 | 420 | - |
| 12 | 11.98334 | 57.66097 | 4.9 | 14.5 | 52.7 | 0.28 | 276.67 | Mean | 100 | 380 | - |
| 13 | 11.97855 | 57.66191 | 4.6 | 17.0 | 59.0 | 0.29 | 183.33 | Mean | 60 | 310 | - |
| 14 | 11.97675 | 57.66153 | 4.7 | 9.0 | 35.9 | 0.25 | 36.67 | Mean | 0 | 120 | - |
| 15 | 11.974 | 57.6604 | 4.2 | 14.7 | 58.0 | 0.25 | 2300 | Mean | 1200 | 2900 | - |
| 16 | 11.96539 | 57.66849 | 3.8 | 15.7 | 67.5 | 0.23 | 172.50 | Mean | 140 | 220 | - |
| 17 | 11.96664 | 57.66607 | 4.2 | 12.5 | 51.8 | 0.24 | 2883.33 | Mean | 1400 | 3400 | - |
| 18 | 11.97045 | 57.66357 | 4.0 | 13.4 | 42.6 | 0.31 | 1490.00 | Mean | 680 | 2200 | - |
| 19 | 11.96859 | 57.66265 | 4.2 | 14.0 | 58.2 | 0.24 | 2641.67 | Mean | 2300 | 2900 | - |
| 20 | 11.97065 | 57.66153 | 4.3 | 12.5 | 51,3 | 0.24 | 3666.67 | Mean | 1500 | 5500 | - |
| 21 | 11.97501 | 57.65861 | 4.1 | 16.8 | 60.4 | 0.28 | 2300.00 | Mean | 2100 | 2600 | - |
| 22 | 11.97351 | 57.65726 | 4.7 | 41.2 | 52.8 | 0.78 | - | Mean | - | - | - |
| 23 | 11.97291 | 57.65711 | 4.2 | 13.7 | 52.6 | 0.26 | 1350.00 | Mean | 400 | 2500 | - |
| 24 | 11.97371 | 57.6554 | 4.4 | 14.9 | 53.6 | 0.28 | 3537.50 | Mean | 2800 | 4100 | - |
| 25 | 11.97407 | 57.65531 | 4.3 | 20.9 | 68.8 | 0.30 | 3354.17 | Mean | 2300 | 4000 | - |
| 26 | 11.97634 | 57.65984 | 4.7 | 9.3 | 31.4 | 0.30 | 95.42 | Mean | 40 | 200 | - |
| 27 | 11.976 | 57.66209 | 4.6 | 7.7 | 31.8 | 0.24 | 281.25 | Mean | 30 | 510 | - |
| 28 | 11.97427 | 57.66398 | 4.3 | 7.8 | 34.0 | 0.23 | 264.17 | Mean | 80 | 390 | - |
| 29 | 11.97285 | 57.66462 | 4.7 | 13.6 | 52.1 | 0.26 | 362.50 | Mean | 160 | 620 | - |
| 30 | 11.97782 | 57.66809 | 4.0 | 14.2 | 54.0 | 0.26 | 610.00 | Mean | 130 | 950 | - |
| 31 | 11.98038 | 57.66634 | 4.5 | 13.1 | 48.5 | 0.27 | 195.50 | Mean | 16 | 360 | - |
| 32 | 11.98132 | 57.66465 | 4.6 | 12.6 | 51.9 | 0.24 | 295.83 | Mean | 170 | 410 | - |
| 33 | 11.97399 | 57.66682 | 4.3 | 9.4 | 37.0 | 0.25 | 195.83 | Mean | 35 | 690 | - |
| 34 | 11.9675 | 57.66443 | 5.4 | 18.8 | 70.2 | 0.27 | 1582.50 | Mean | 540 | 3000 | - |
| 35 | 11.96243 | 57.66394 | 4.5 | 21.6 | 83.4 | 0.26 | 561.67 | Mean | 100 | 1200 | - |
| 36 | 11.9618 | 57.66294 | 4.2 | 14.3 | 59.2 | 0.24 | 1087.50 | Mean | 940 | 1400 | - |
| 37 | 11.96266 | 57.66258 | 4.3 | 15.2 | 57.3 | 0.26 | 1358.33 | Mean | 1100 | 1600 | - |
| 38 | 11.96467 | 57.66021 | 3.7 | 14.1 | 56.2 | 0.25 | 193.33 | Mean | 140 | 240 | - |
| 39 | 11.96337 | 57.65794 | 4.0 | 14.2 | 56.2 | 0.25 | 2800.00 | Mean | 1700 | 3500 | - |
| 40 | 11.96511 | 57.65685 | 3.8 | 10.6 | 51.3 | 0.21 | 596.67 | Mean | 50 | 1600 | - |
| 41 | 11.96741 | 57.65724 | 3.9 | 10.2 | 41.7 | 0.24 | 4158.33 | Mean | 3600 | 5000 | - |

| | | | | | | | | | | | |
|---|---|---|---|---|---|---|---|---|---|---|---|
| 42 | 11.96765 | 57.65976 | 3.8 | 12.3 | 59.5 | 0.21 | 605.83 | Mean | 30 | 1600 | - |
| 43 | 11.96716 | 57.66119 | 4.3 | 14.3 | 53.2 | 0.27 | 2475.00 | Mean | 1800 | 3000 | - |
| 44 | 11.96675 | 57.66242 | 3.9 | 12.9 | 54.3 | 0.24 | 2000.83 | Mean | 550 | 3000 | - |
| 45 | 11.96666 | 57.66411 | 4.8 | 17.4 | 71.0 | 0.25 | 2391.67 | Mean | 2000 | 2800 | - |
| 46 | 11.95588 | 57.67946 | 3.8 | 14.8 | 58.8 | 0.25 | 2058.33 | Mean | 2000 | 2800 | - |
| 47 | 11.95557 | 57.67815 | 4.1 | 14.3 | 56.7 | 0.25 | 1130.83 | Mean | 1500 | 1800 | - |
| 48 | 11.95348 | 57.67791 | 5.2 | 11.0 | 34.9 | 0.31 | 630.00 | Mean | 760 | 760 | - |
| 49 | 11.95401 | 57.67607 | 4.8 | 12.7 | 61.4 | 0.21 | 26.25 | Mean | 40 | 40 | - |
| 50 | 11.9565 | 57.67247 | 4.5 | 12.4 | 49.5 | 0.25 | 3375.00 | Mean | 3000 | 4100 | - |
| 51 | 11.95743 | 57.65568 | 4.5 | 15.0 | 66.8 | 0.22 | 416.67 | Mean | 310 | 500 | - |
| 52 | 11.95536 | 57.65871 | 4.4 | 14.8 | 65.3 | 0.23 | 559.17 | Mean | 430 | 1200 | - |
| 53 | 11.95441 | 57.66075 | 4.2 | 13.4 | 61.4 | 0.22 | 318.33 | Mean | 300 | 490 | - |
| 54 | 11.9584 | 57.66065 | 4.0 | 13.4 | 51.7 | 0.26 | 11.25 | Mean | 25 | 25 | - |
| 55 | 11.95998 | 57.66113 | 4.2 | 13.2 | 51.0 | 0.26 | 3091.67 | Mean | 3100 | 3700 | - |
| 56 | 11.97349 | 57.65908 | 4.3 | 14.8 | 54.1 | 0.27 | 1575.00 | Mean | 1500 | 2000 | - |
| 17ANH001 | 11.97282 | 57.67169 | 4.7 | 13.0 | 49.3 | 0.26 | 200 | Median | 150 | 300 | - |
| 17ANH002 | 11.97164 | 57.67126 | 4.1 | 13.2 | 51.0 | 0.26 | 100 | Median | 20 | 300 | - |
| 17ANH003 | 11.97123 | 57.67157 | 4.2 | 12.9 | 45.4 | 0.28 | 200 | Median | 50 | 300 | - |
| 17ANH004 | 11.971 | 57.67052 | 4.0 | 10.4 | 49.0 | 0.21 | 200 | Median | 100 | 300 | - |
| 17ANH005 | 11.97123 | 57.67015 | 4.3 | 14.3 | 53.1 | 0.27 | 100 | Median | 50 | 200 | - |
| 17ANH006 | 11.9716 | 57.6695 | 4.0 | 13.7 | 47.8 | 0.29 | 200 | Median | 50 | 300 | - |
| 17ANH007 | 11.97132 | 57.66795 | 4.2 | 9.5 | 36.0 | 0.26 | 450 | Median | 400 | 500 | - |
| 17ANH008 | 11.9705 | 57.66778 | 4.3 | 8.5 | 28.1 | 0.30 | 300 | Median | 100 | 650 | - |
| 17ANH009 | 11.96896 | 57.66772 | 4.6 | 9.4 | 53.9 | 0.17 | 2500 | Median | 1800 | 3500 | - |
| 17ANH010 | 11.96773 | 57.66708 | 3.9 | 16.1 | 56.2 | 0.29 | 62 | Median | 60 | 70 | - |
| 17ANH011 | 11.96625 | 57.6674 | 3.8 | 4.6 | 16.8 | 0.28 | 400 | Median | 300 | 800 | - |
| 17ANH012 | 11.96509 | 57.66671 | 4.3 | 12.8 | 57.7 | 0.22 | 370 | Median | 100 | 500 | - |
| 17ANH013 | 11.96334 | 57.66642 | 3.8 | 13.3 | 52.5 | 0.25 | 1000 | Median | 300 | 2500 | - |
| 17ANH014 | 11.96434 | 57.66927 | 4.0 | 10.5 | 53.1 | 0.20 | 200 | Median | 100 | 400 | - |
| 17ANH015 | 11.96536 | 57.66843 | 3.9 | 15.7 | 67.6 | 0.23 | 200 | Median | 100 | 300 | - |
| 17ANH016 | 11.96613 | 57.66878 | 5.3 | 22.1 | 82.1 | 0.27 | 50 | Median | 40 | 85 | - |
| 17ANH017 | 11.96696 | 57.6699 | 5.9 | 10.1 | 36.3 | 0.28 | 1000 | Median | 600 | 2000 | - |
| 17ANH018 | 11.96715 | 57.6718 | 4.8 | 15.5 | 37.6 | 0.41 | 450 | Median | 100 | 800 | - |
| 17ANH019 | 11.96066 | 57.66708 | 3.7 | 12.1 | 51.9 | 0.23 | 800 | Median | 500 | 3000 | - |
| 17ANH020 | 11.96184 | 57.66567 | 4.1 | 14.1 | 57.7 | 0.24 | 70 | Median | 60 | 150 | - |
| 17ANH021 | 11.96072 | 57.66472 | 3.5 | 11.9 | 58.7 | 0.20 | 800 | Median | 400 | 1000 | - |
| 17ANH022 | 11.95883 | 57.66367 | 4.4 | 14.2 | 58.5 | 0.24 | 3000 | Median | 1500 | 3500 | - |
| 17ANH023 | 11.95859 | 57.66403 | 4.2 | 13.8 | 52.3 | 0.26 | 3000 | Median | 1500 | 3500 | - |
| 17ANH024 | 11.95749 | 57.66443 | 4.5 | 7.7 | 47.4 | 0.16 | 5000 | Median | 3500 | 6000 | - |
| 17ANH025 | 11.95613 | 57.66545 | 3.9 | 11.9 | 49.8 | 0.24 | 70 | Median | 40 | 300 | - |
| 17ANH026 | 11.95707 | 57.66592 | 5.5 | 19.5 | 83.2 | 0.23 | 400 | Median | 100 | 800 | - |
| 17ANH027 | 11.95599 | 57.66676 | 2.2 | 9.2 | 31.2 | 0.30 | 3000 | Median | 900 | 6000 | - |
| 17ANH028 | 11.95517 | 57.66668 | 4.2 | 13.2 | 52.5 | 0.25 | 2000 | Median | 700 | 2500 | - |
| 17ANH029 | 11.95347 | 57.66555 | 5.2 | 19.9 | 70.5 | 0.28 | 50 | Median | 50 | 60 | - |
| 17ANH030 | 11.95285 | 57.66493 | 6.1 | 22.8 | 84.1 | 0.27 | 150 | Median | 70 | 200 | - |
| 17ANH031 | 11.95164 | 57.66491 | 4.3 | 10.7 | 61.0 | 0.18 | 55 | Median | 50 | 100 | - |
| 17ANH032 | 11.95198 | 57.66402 | 4.6 | 17.3 | 65.9 | 0.26 | 500 | Median | 400 | 600 | - |
| 17ANH033 | 11.953 | 57.66265 | 4.7 | 16.8 | 62.7 | 0.27 | 400 | Median | 200 | 600 | - |
| 17ANH034 | 11.95177 | 57.66211 | 5.6 | 18.7 | 82.7 | 0.23 | 400 | Median | 150 | 600 | - |
| 17ANH035 | 11.94956 | 57.66204 | 4.3 | 9.3 | 46.0 | 0.20 | 45 | Median | 40 | 50 | - |
| 17ANH036 | 11.94697 | 57.66049 | 4.6 | 1.3 | 5.6 | 0.24 | 45 | Median | 10 | 65 | - |
| 17ANH037 | 11.94619 | 57.6611 | 4.6 | 1.9 | 6.1 | 0.32 | 70 | Median | 65 | 85 | - |

| | | | | | | | | | | | |
|---|---|---|---|---|---|---|---|---|---|---|---|
| 17ANH038 | 11.94668 | 57.66311 | 4.6 | 3.8 | 22.3 | 0.17 | 700 | Median | 400 | 1500 | - |
| 17ANH039 | 11.94745 | 57.66398 | 4.6 | 7.4 | 35.8 | 0.21 | 60 | Median | 40 | 80 | - |
| 17ANH040 | 11.95018 | 57.66393 | 4.3 | 13.3 | 59.2 | 0.22 | 500 | Median | 400 | 600 | - |
| 17ANH041 | 11.95065 | 57.66289 | 4.3 | 14.2 | 61.2 | 0.23 | 500 | Median | 400 | 600 | - |
| 17ANH042 | 11.95438 | 57.66204 | 4.3 | 17.2 | 60.3 | 0.29 | 450 | Median | 200 | 500 | - |
| 17ANH043 | 11.95549 | 57.66203 | 5.7 | 21.6 | 80.0 | 0.27 | 150 | Median | 100 | 200 | - |
| 17ANH044 | 11.95576 | 57.66324 | 4.5 | 5.3 | 27.9 | 0.19 | 6000 | Median | 500 | 6500 | - |
| 17ANH045 | 11.95469 | 57.66467 | 0.8 | 41.5 | 43.5 | 0.95 | 80 | Median | 60 | 150 | - |
| 17ANH046 | 11.95888 | 57.658 | 3.7 | 10.3 | 47.6 | 0.22 | 600 | Median | 400 | 900 | - |
| 17ANH047 | 11.95959 | 57.66674 | 3.9 | 15.0 | 69.8 | 0.22 | 4500 | Median | 4000 | 5000 | - |
| 17ANH048 | 11.96046 | 57.66835 | 4.0 | 11.9 | 47.1 | 0.25 | 800 | Median | 400 | 2000 | - |
| 17ANH049 | 11.9651 | 57.66752 | 4.0 | 7.9 | 47.7 | 0.17 | 600 | Median | 400 | 800 | - |
| 17ANH050 | 11.96895 | 57.66944 | 3.8 | 6.5 | 24.1 | 0.27 | 400 | Median | 300 | 1000 | - |
| 17ANH051 | 11.96856 | 57.67107 | 4.8 | 11.9 | 34.2 | 0.35 | 450 | Median | 100 | 800 | - |
| 17ANH052 | 11.96316 | 57.67864 | 2.9 | 15.2 | 13.0 | 1.17 | 600 | Median | 400 | 800 | - |
| 17ANH053 | 11.96284 | 57.67897 | 4.6 | 7.1 | 35.3 | 0.20 | 450 | Median | 200 | 550 | - |
| 17ANH054 | 11.96271 | 57.67824 | 4.6 | 7.7 | 34.0 | 0.23 | 350 | Median | 200 | 400 | - |
| 17ANH055 | 11.96249 | 57.67973 | 4.4 | 7.2 | 32.8 | 0.22 | 1500 | Median | 800 | 2000 | - |
| 17ANH056 | 11.96277 | 57.67992 | 4.3 | 8.9 | 35.3 | 0.25 | 150 | Median | 100 | 250 | - |
| 17ANH057 | 11.96342 | 57.67996 | 4.8 | 10.3 | 39.5 | 0.26 | 700 | Median | 200 | 2000 | - |
| 17ANH058 | 11.96427 | 57.67956 | 4.4 | 15.4 | 48.8 | 0.32 | 100 | Median | 60 | 300 | - |
| 17ANH059 | 11.96533 | 57.67927 | 4.1 | 11.8 | 46.2 | 0.26 | 2000 | Median | 1500 | 3000 | - |
| 17ANH060 | 11.96482 | 57.67874 | 2.8 | 18.8 | 15.6 | 1.20 | 1500 | Median | 700 | 2000 | - |
| 17ANH061 | 11.96599 | 57.67818 | 4.0 | 11.6 | 45.2 | 0.26 | 700 | Median | 400 | 2000 | - |
| 17ANH062 | 11.9641 | 57.67924 | 4.3 | 16.5 | 53.8 | 0.31 | 4500 | Median | 4000 | 5000 | - |
| 17ANH063 | 11.96391 | 57.6787 | 4.1 | 8.0 | 34.6 | 0.23 | 4000 | Median | 600 | 6000 | - |
| 17ANH064 | 11.96363 | 57.67808 | 4.8 | 7.7 | 36.5 | 0.21 | 4000 | Median | 3000 | 4500 | - |
| 17ANH065 | 11.96519 | 57.67756 | 4.3 | 12.8 | 54.4 | 0.23 | 500 | Median | 400 | 700 | - |
| 17ANH066 | 11.96455 | 57.67698 | 4.4 | 7.4 | 32.5 | 0.23 | 450 | Median | 350 | 800 | - |
| 17ANH067 | 11.9654 | 57.67647 | 4.6 | 9.1 | 36.3 | 0.25 | 450 | Median | 250 | 800 | - |
| 17ANH068 | 11.9662 | 57.67625 | 4.5 | 9.4 | 37.7 | 0.25 | 500 | Median | 400 | 600 | - |
| 17ANH069 | 11.96605 | 57.67577 | 4.5 | 10.0 | 35.8 | 0.28 | 80 | Median | 60 | 85 | - |
| 17ANH070 | 11.96713 | 57.67554 | 4.1 | 14.4 | 48.8 | 0.29 | 100 | Median | 100 | 150 | - |
| 17ANH071 | 11.9673 | 57.67622 | 4.3 | 12.2 | 48.7 | 0.25 | 50 | Median | 40 | 60 | - |
| 17ANH072 | 11.96723 | 57.67677 | 4.1 | 12.3 | 46.1 | 0.27 | 4500 | Median | 2000 | 8000 | - |
| 17ANH073 | 11.96625 | 57.6771 | 4.0 | 12.7 | 48.4 | 0.26 | 2000 | Median | 1000 | 3000 | - |
| 17ANH074 | 11.96663 | 57.67787 | 4.0 | 9.3 | 39.0 | 0.24 | 800 | Median | 600 | 1500 | - |
| 17ANH075 | 11.96824 | 57.67657 | 4.5 | 9.9 | 46.4 | 0.21 | 300 | Median | 200 | 400 | - |
| 17ANH076 | 11.9672 | 57.67384 | 4.2 | 11.6 | 51.7 | 0.23 | 2000 | Median | 1500 | 2500 | - |
| 17ANH077 | 11.96343 | 57.67221 | 5.6 | 9.6 | 31.3 | 0.31 | 60 | Median | 40 | 200 | - |
| 17ANH078 | 11.96363 | 57.67113 | 4.4 | 12.4 | 28.9 | 0.43 | 400 | Median | 200 | 1000 | - |
| 17ANH079 | 11.95972 | 57.67016 | 3.9 | 17.6 | 75.1 | 0.23 | 200 | Median | 150 | 300 | - |
| 17ANH080 | 11.95797 | 57.66917 | 4.1 | 10.8 | 43.4 | 0.25 | 100 | Median | 20 | 300 | - |
| 17ANH081 | 11.95818 | 57.66808 | 4.1 | 14.0 | 51.3 | 0.27 | 200 | Median | 50 | 300 | - |
| 17ANH082 | 11.9555 | 57.66898 | 4.2 | 11.6 | 42.8 | 0.27 | 200 | Median | 100 | 300 | - |
| 17ANH083 | 11.95268 | 57.66911 | 4.2 | 5.8 | 22.6 | 0.26 | 100 | Median | 50 | 200 | - |
| 17ANH084 | 11.95275 | 57.66742 | 3.5 | 6.0 | 23.2 | 0.26 | 200 | Median | 50 | 300 | - |
| 17ANH085 | 11.95051 | 57.66728 | 4.5 | 15.0 | 63.5 | 0.24 | 450 | Median | 400 | 500 | - |
| 17ANH086 | 11.95062 | 57.66628 | 4.0 | 15.5 | 60.2 | 0.26 | 300 | Median | 100 | 650 | - |
| 17ANH087 | 11.94882 | 57.66623 | 4.3 | 13.8 | 60.2 | 0.23 | 2500 | Median | 1800 | 3500 | - |
| 17ANH088 | 11.94977 | 57.66472 | 4.6 | 12.4 | 62.2 | 0.20 | 62 | Median | 60 | 70 | - |
| 17ANH089 | 11.94776 | 57.66481 | 1.9 | 4.5 | 18.5 | 0.24 | 400 | Median | 300 | 800 | - |

| | | | | | | | | | | | |
|---|---|---|---|---|---|---|---|---|---|---|---|
| 17ANH090 | 11.94705 | 57.66553 | 1.2 | 1.4 | 6.3 | 0.22 | 370 | Median | 100 | 500 | - |
| 17ANH091 | 11.95235 | 57.66621 | 6.2 | 16.5 | 80.3 | 0.21 | 1000 | Median | 300 | 2500 | - |
| 17ANH092 | 11.95446 | 57.66661 | 4.5 | 13.4 | 50.7 | 0.26 | 200 | Median | 100 | 400 | - |
| 17ANH093 | 11.95578 | 57.66769 | 4.5 | 14.2 | 66.9 | 0.21 | 200 | Median | 100 | 300 | - |
| 17ANH094 | 11.95737 | 57.67017 | 4.2 | 14.6 | 58.4 | 0.25 | 50 | Median | 40 | 85 | - |
| 17ANH095 | 11.96263 | 57.6702 | 4.2 | 7.7 | 34.6 | 0.22 | 1000 | Median | 600 | 2000 | - |
| 17ANH096 | 11.96472 | 57.67036 | 4.5 | 8.2 | 26.4 | 0.31 | 450 | Median | 100 | 800 | - |
| 17ANH097 | 11.96522 | 57.67086 | 4.1 | 8.2 | 27.8 | 0.30 | 800 | Median | 500 | 3000 | - |
| 17ANH098 | 11.96468 | 57.6742 | 4.6 | 12.8 | 42.9 | 0.30 | 70 | Median | 60 | 150 | - |
| 17ANH099 | 11.96239 | 57.67392 | 4.7 | 9.3 | 30.9 | 0.30 | 800 | Median | 400 | 1000 | - |
| 17ANH100 | 11.9618 | 57.67444 | 4.7 | 6.4 | 26.0 | 0.25 | 3000 | Median | 1500 | 3500 | - |
| 17ANH101 | 11.95763 | 57.67613 | 4.3 | 13.8 | 55.8 | 0.25 | 3000 | Median | 1500 | 3500 | - |
| A001 | 11.96675 | 57.68887 | 2.7 | 2.8 | 9.4 | 0.30 | - | - | - | - | - |
| A002 | 11.96675 | 57.68887 | 6.4 | 1.4 | 4.0 | 0.35 | - | - | - | - | - |
| A003 | 11.96752 | 57.68901 | 2.2 | 1.2 | 6.9 | 0.17 | - | - | - | - | - |
| A004 | 11.96622 | 57.68954 | 1.7 | 0.7 | 5.5 | 0.13 | - | - | - | - | - |
| A005 | 11.96493 | 57.68912 | 2.7 | 4.7 | 16.0 | 0.29 | - | - | - | - | - |
| A006 | 11.96506 | 57.68937 | 2.9 | 1.8 | 2.9 | 0.60 | - | - | - | - | - |
| A007 | 11.96565 | 57.68741 | 1.8 | 1.5 | 6.8 | 0.21 | - | - | - | - | - |
| A008 | 11.96690 | 57.68755 | 2.8 | 1.7 | 14.7 | 0.12 | - | - | - | - | - |
| A009 | 11.96776 | 57.68835 | 1.6 | 0.6 | 5.7 | 0.11 | - | - | - | - | - |
| A010 | 11.96870 | 57.68790 | 2.1 | 1.7 | 10.8 | 0.16 | - | - | - | - | - |
| A011 | 11.96733 | 57.68707 | 2.4 | 2.2 | 8.3 | 0.26 | - | - | - | - | - |
| 17FF12 | 11.97142 | 57.68778 | 1.6 | 1.5 | 5.5 | 0.28 | - | - | - | - | - |
| 17FF13 | 11.97145 | 57.68758 | 1.7 | 1.4 | 7.2 | 0.19 | - | - | - | - | - |
| 17FF163 | 11.96612 | 57.68992 | 2.2 | 0.8 | 7.5 | 0.11 | - | - | - | - | - |
| 17FF164 | 11.96597 | 57.68973 | 2.7 | 1.4 | 11.6 | 0.12 | - | - | - | - | - |
| 18FF146 | 11.97012 | 57.69064 | 3.4 | 4.0 | 11.7 | 0.34 | - | - | - | - | - |
| 18FF147 | 11.96054 | 57.68670 | 3.2 | 1.7 | 8.7 | 0.20 | - | - | - | - | - |
| 18FF148 | 11.95992 | 57.68600 | 2.7 | 2.3 | 7.2 | 0.32 | - | - | - | - | - |
| 18FF149 | 11.96087 | 57.68684 | 2.7 | 3.0 | 13.0 | 0.23 | - | - | - | - | - |
| 18FF150 | 11.96101 | 57.68668 | 2.5 | 2.7 | 10.6 | 0.26 | - | - | - | - | - |
| 18FF151 | 11.96105 | 57.68655 | 2.5 | 3.3 | 8.7 | 0.38 | - | - | - | - | - |
| 18FF152 | 11.96083 | 57.68642 | 1.3 | 2.8 | 7.3 | 0.39 | - | - | - | - | - |
| 18FF153 | 11.96065 | 57.68645 | 1.8 | 2.7 | 6.3 | 0.43 | - | - | - | - | - |
| 18FF159 | 11.96041 | 57.68637 | 2.4 | 1.8 | 6.8 | 0.27 | - | - | - | - | - |
| 18FF155 | 11.96058 | 57.68620 | 2.7 | 1.7 | 6.7 | 0.26 | - | - | - | - | - |
| 18FF156 | 11.96063 | 57.68628 | 2.5 | 2.1 | 6.5 | 0.32 | - | - | - | - | - |
| 18FF157 | 11.96069 | 57.68612 | 2.6 | 1.7 | 7.3 | 0.23 | - | - | - | - | - |
| 18FF158 | 11.96134 | 57.68616 | 2.6 | 1.8 | 7.4 | 0.24 | - | - | - | - | - |
| 18FF159 | 11.96130 | 57.68627 | 1.6 | 1.4 | 4.6 | 0.31 | - | - | - | - | - |
| 18FF160 | 11.96150 | 57.68628 | 2.4 | 2.0 | 6.4 | 0.32 | - | - | - | - | - |
| 18FF161 | 11.96158 | 57.68612 | 2.4 | 2.0 | 6.8 | 0.30 | - | - | - | - | - |
| 18FF162 | 11.96178 | 57.68604 | 2.5 | 2.0 | 7.1 | 0.29 | - | - | - | - | - |
| 18FF163 | 11.96087 | 57.68597 | 2.5 | 2.5 | 7.1 | 0.35 | - | - | - | - | - |
| 18FF164 | 11.96072 | 57.68575 | 4.5 | 4.6 | 8.6 | 0.53 | - | - | - | - | - |
| 18FF165 | 11.96048 | 57.68579 | 3.2 | 3.8 | 9.3 | 0.41 | - | - | - | - | - |
| 18FF166 | 11.96202 | 57.68591 | 2.6 | 2.1 | 7.4 | 0.28 | - | - | - | - | - |
| 18FF167 | 11.96214 | 57.68475 | 9.8 | 13.9 | 123.2 | 0.11 | - | - | - | - | - |
| 18FF168 | 11.96255 | 57.68505 | 4.1 | 6.8 | 25.9 | 0.26 | - | - | - | - | - |
| 18FF169 | 11.96432 | 57.68612 | 3.3 | 3.1 | 14.1 | 0.22 | - | - | - | - | - |
| 18FF170 | 11.96430 | 57.68643 | 2.7 | 4.8 | 9.3 | 0.52 | - | - | - | - | - |

| | | | | | | | | | | | |
|---|---|---|---|---|---|---|---|---|---|---|---|
| 18FF171 | 11.96445 | 57.68682 | 3.0 | 4.3 | 13.3 | 0.32 | - | - | - | - | - |
| 19FF001 | 11.96231 | 57.68581 | 3.1 | 3.9 | 11.8 | 0.33 | - | - | - | - | - |
| 19FF002 | 11.96230 | 57.68609 | 3.8 | 3.1 | 10.8 | 0.28 | - | - | - | - | - |
| 19FF003 | 11.96158 | 57.68660 | 3.2 | 5.3 | 14.9 | 0.36 | - | - | - | - | - |
| 16FF200 | 11.961608 | 57.684195 | 6.6 | 16.5 | 100.0 | 0.16 | - | - | - | - | - |
| 17FF161 | 11.968533 | 57.6737167 | 4.2 | 11.2 | 46.4 | 0.24 | - | - | - | - | - |
| 17FF162 | 11.9673833 | 57.6742167 | 3.8 | 8.1 | 56.2 | 0.14 | - | - | - | - | - |
| 19FF097 | 11.95755 | 57.68497 | 5.5 | 14.1 | 74.0 | 0.19 | - | - | - | - | - |
| 19FF099 | 11.95664 | 57.68511 | 5.7 | 12.9 | 40.3 | 0.32 | - | - | - | - | - |
| 19FF100 | 11.95588 | 57.6855 | 5.8 | 21.2 | 75.2 | 0.28 | - | - | - | - | - |
| 19FF101 | 11.96138 | 57.68443 | 6.3 | 12.5 | 78.6 | 0.16 | - | - | - | - | - |
| 19FF108 | 11.95627 | 57.6861 | 6.3 | 22.7 | 78.6 | 0.29 | - | - | - | - | - |
| 19FF107 | 11.95615 | 57.68636 | 3.4 | 9.5 | 65.1 | 0.15 | - | - | - | - | - |

D. Scanned thin sections. The red dots mark where photos have been taken with a microscope.

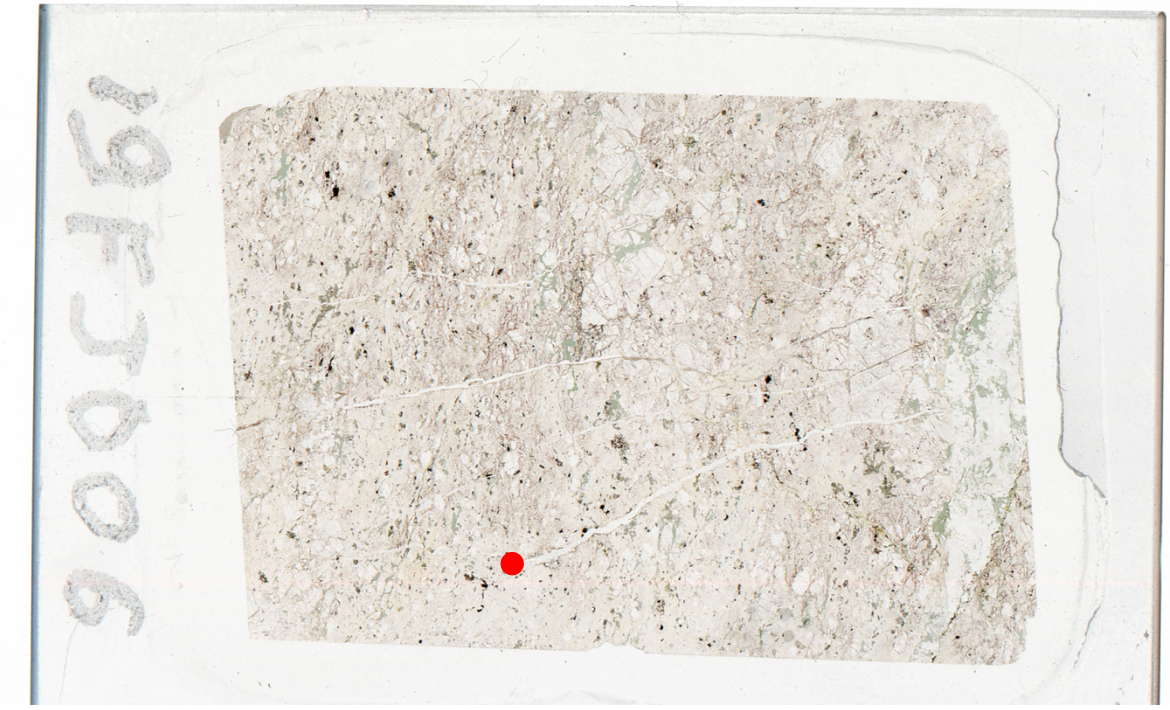

E. Table of all rock samples taken in Änggårdsbergen for the study of the RA-granite.

| Sample ID | Lon. | Lat. | Collected by | Sample type |
|---|---|---|---|---|
| 16FF200 | 11.961608 | 57.684195 | Prof. Erik Sturkell | Geochemical analysis and microscopy |
| 17ANH009 | 11.968959 | 57.667717 | Hultin & Håkansson, 2018 | Geochemical analysis and microscopy |
| 17ANH030 | 11.952856 | 57.66493 | Hultin & Håkansson, 2018 | Microscopy |
| 17FF02 | 11.950431 | 57.67403 | Prof. Erik Sturkell | Geochemical analysis and microscopy |
| 17FF04 | 11.964946 | 57.669769 | Prof. Erik Sturkell | Geochemical analysis and microscopy |
| 18AJE1 | 11.972481 | 57.664701 | Cooper Svensson & Lundin Frisk, 2018 | Microscopy |
| 18AJE2 | 11.967478 | 57.664563 | Cooper Svensson & Lundin Frisk, 2018 | Geochemical analysis and microscopy |
| 18AJE3 | 11.960791 | 57.664303 | Cooper Svensson & Lundin Frisk, 2018 | Geochemical analysis |
| 18AJE4 | 11.956604 | 57.664634 | Cooper Svensson & Lundin Frisk, 2018 | Geochemical analysis and microscopy |
| 18AJE5 | 11.951442 | 57.66459 | Cooper Svensson & Lundin Frisk, 2018 | Microscopy |
| 18AJE6 | 11.950403 | 57.664574 | Cooper Svensson & Lundin Frisk, 2018 | Geochemical analysis and microscopy |
| 19FJ001 | 11.956104 | 57.683398 | Elf & Winberg, 2019 | Geochemical analysis and microscopy |
| 19FJ006 | 11.9629 | 57.684397 | Elf & Winberg, 2019 | Geochemical analysis and microscopy |
| 19FJ055 | 11.968541 | 57.67372 | Prof. Erik Sturkell | Geochemical analysis |
| 19FJ056 | 11.957613 | 57.684009 | Elf & Winberg, 2019 | Geochemical analysis |